Cover Page

ALPHA FOUNDATION FOR THE IMPROVEMENT OF MINE SAFETY AND HEALTH

Final Technical Report

Project Title: Development of Guidance for The Selection and Use of Atmospheric Monitoring Systems to Improve Decision-Making during Routine and Post-Accident Operations

Grant Number: AFC215-01

Organization: The Pennsylvania State University

Principal Investigators:

Shimin Liu, Ph.D.
Associate Professor of Mining Engineering
Department of Energy and Mineral Engineering
The Pennsylvania State University

Jeffery L. Kohler, Ph.D.
Professor of Mining Engineering (retired),
Department of Energy and Mineral Engineering
The Pennsylvania State University

Long Fan
Graduate Research Assistant in Mining Engineering
Department of Energy and Mineral Engineering
The Pennsylvania State University

Edward Zeglen, P.E.
Chief Ventilation Engineer (retired)
Cumberland Mine
Alpha Natural Resources

Contact Information :

Phone : 814-863-4491
Fax : 814-865-3248
E-mail : szl3@psu.edu

Period of Performance: September 1, 2015 to July 31, 2019

Acknowledgement/Disclaimer: This study was sponsored by the Alpha Foundation for the Improvement of Mine Safety and Health, Inc. (ALPHA FOUNDATION). The views, opinions and recommendations expressed herein are solely those of the authors and do not imply any endorsement by the ALPHA FOUNDATION, its Directors and staff.

Table of Content

List of Figures

List of Tables

1.0 Executive Summary

The potential of mine-wide monitoring systems to improve mine safety and health has been recognized for decades, yet the deployment of these systems for such purposes has been extremely limited in the U.S. and globally. Although not perfect, the technologies to enable mine-wide atmospheric monitoring systems (AMS) have been commercially available, and technology itself has not been the greatest barrier to widespread adoption of these systems. Rather, it has been a lack of knowledge on where the sensors will be placed and how the resulting information will be used to achieve specific safety or health outcomes.

The ongoing challenges and costs associated with acquiring AMS information are significant, and they underscore the need for a purposeful strategy for every installed sensor. The difficulty in actually using the large quantities of data to improve decision-making at the mine is a persistent problem. The question of what to do with the data generated by these systems is as difficult to answer today as it was thirty years ago. While large graphical displays of sensor values superimposed on maps and diagrams appear impressive, the practical use of this information to improve safety and health (S&H) outcomes is another matter.

The current state of technology makes it easier to incorporate a greater number of sensors, which will likely produce even larger quantities of data, thus creating an even greater risk that meaningful information will be obscured. Furthermore, the interest in employing backup measures, such as tube bundle systems, to improve post-accident functionality increases the complexity of the problem. Mine operators need practical guidance on the selection and location of sensors to achieve defined safety goals, as well as guidance on how to align the performance characteristics of the monitoring system with those safety goals.

The selection and configuration of AMS for routine and post-accident functionality must be based on a logical construct specifying how information will be used to improve safety. The purposeful use of atmospheric monitoring will facilitate the detection of potentially hazardous conditions as they begin to develop; this process requires definitive guidance to align sensor selection and location with decision-making requirements. The overarching goal of this project was to provide practical guidelines for improving mine safety through the strategic placement of sensors in AMS.

This objective was pursued by achieving three specific aims. The first was to define the information needs to support decision-making during routine operations; the second was to define the salient characteristics of monitoring systems that could provide the information so identified; and the third was to utilize the findings to prepare practical, “how-to” guidance for mine personnel. The research methods used to achieve the project objective included the following: interviews with mining personnel (e.g., mine foremen, ventilation engineers, mine engineers, face bosses, fire bosses, and inspectors) to understand their decision-making processes and information requirements; ventilation modeling and simulations to study relationships between the placement of a sensor and the usefulness of the data generated to inform decisions about potentially hazardous situations; and on-site validations.

This project focused on underground coal mines and the resulting guidelines are primarily intended for underground coal mine operators. Notwithstanding, the underlying strategy can be adapted to noncoal mines. The two main outcomes of this research were the location strategy for the detection of developing problems in the mine ventilation systems, and the rationale for using pressure transducers rather than air velocity sensors to establish volumetric airflow rates.

2.0 Problem Statement and Objective

Focus area: Health and Safety Interventions

Topic Areas: Monitoring Systems and Integrated Control Technologies

2.1 Problem Statement

The potential of atmospheric monitoring systems (AMS) [1] to improve safety has been recognized for decades (Kohler,1992). The 2006 Sago Mine disaster and its aftermath underscored the potential of technology to improve mine safety. Subsequently, the MINER Act of 2006 spurred significant technological advances and substantial federal funding for the development of the requisite technologies. Mines installed sophisticated node and mesh-based communications backbones that could support mine-wide monitoring of all major systems including ventilation. There was much excitement throughout the mining community over the possibilities. Monitoring capability increased as a result of the more capable communication backbones that had been installed. The focus, however, was on monitoring production-related parameters and machine conditions, with far less attention given to monitoring ventilation parameters such as airflow and methane concentration[2].

The Upper Big Branch Mine explosion in 2010 highlighted the need to use mine monitoring systems to detect potentially hazardous conditions because it was widely believed that the deleterious conditions that preceded the explosion could have been detected with an AMS. A legislative attempt to modify the MINER Act and require atmospheric monitoring failed. Subsequently, Alpha Natural Resources (ANR) agreed to install AMS in all of its mines as part of a Non-Prosecution Agreement (NPA) with the U.S. government when it purchased the Upper Big Branch Mine and other assets of Massey Energy.

Within a few years, ANR, working with Matrix, Inc., developed and installed AMS in many of its mines. The technical performance of these systems was excellent, but the age-old problems of where to locate the sensors and how to utilize the collected data persisted. One of the authors of this report (Kohler) was involved in those discussions, and as a consequence, a proposal was developed to address those problems and submitted for consideration to the Alpha Foundation. The findings presented in this report are based on the funded project begun by that proposal.

Researchers are currently pursuing solutions to a number of important problems involving AMS. One of the more important sets of problems concerns data analytics and the best uses of the enormous quantity of data produced by the equipment and systems found in today's mines (Agioutantus, 2014). Another is the use of artificial intelligence to make intelligent decisions without the involvement of engineering or operations personnel. The robust communication (digital data) networks available in many mines allow for the placement of a virtually unlimited number of sensors throughout the mine. The very thought of knowing, in real time, a collection of ventilation parameters that includes airflow rates and gas concentrations at any location in the mine generates much enthusiasm for the potential of these technologies to improve safety as well

[1] Refer to Section 3.0 (Research Approach) for clarification of the use of the term *atmospheric monitoring systems (AMS)* for the purposes of this report.

[2] Methane monitoring is not the focus of the project, instead the project tried to use pressure monitoring strategy to inform the critical change of the ventilation system. Refer to Section 4.1.2 (Sensor Inputs) for the justification of the superiority of pressure monitoring over air velocity monitoring.

as productivity. Great interest also surrounds the prospect of endowing AMS with the expertise of seasoned ventilation engineers so that the monitored parameters can be utilized to realize their safety and production potential. Continued research into the attendant data analytics and artificial intelligence challenges is key to realizing these prospects, which will likely take several more years. In the meantime, there is a need to achieve lifesaving benefits through atmospheric monitoring as simply as practicable. That is the goal of this project.

Why this need for simplicity? Despite the potential of AMS technology and the many attempts to employ it over the past 40 years, the industry continues to shun it. The two oft-cited reasons for this reluctance are the purported impossibility of using the "reams of data" from the AMS and the challenge of maintaining a large number of sensors. These reasons impeded the adoption of the available technology in 1980 and continue to do so today (Kohler 1987). The initial cost of sensors is not trivial, but the more significant costs derive from the labor needed to inspect and calibrate these sensors and to maintain records of these activities. Therefore, the focus of the work here was to reduce the number of sensors to the smallest number that yields sufficient information to support decision-making. As a prerequisite step, it was necessary to identify the types of decisions that would need to be informed by these sensors.

The set of decisions for this project was limited to those surrounding the identification of hazardous or developing and potentially hazardous conditions. What events and scenarios lead to these potentially hazardous conditions, and what information would be required to detect these conditions? In essence, the challenges were to define a set of event scenarios that could lead to hazardous conditions and then to identify the smallest number of sensors or locations that could serve as sentinels to alert mine personnel to the need for closer examination[3]. Of course, mine monitoring systems from the earliest days to the present have had the ability to "alarm" when sensor values moved outside of preset ranges. However, this function proved to be of little value: false alarms were quite common, and the size of the dead bands set around trigger threshold were often excessive. This project aims to overcome these past limitations by reducing the number of installed sensors and facilitating more purposeful placement. Additionally, the issue of false alarms and trigger thresholds is addressed.

2.2 Project Research Objectives

The selection and configuration of AMS for routine and post-accident functionality must be based on a logical construct specifying how information will be used to improve safety. The purposeful use of atmospheric monitoring will facilitate the detection of potentially hazardous conditions as they begin to develop; this process requires definitive guidance to align sensor selection and location with decision-making requirements. The overarching ***objective*** of this project was to provide practical guidelines for improving mine safety through the strategic placement of sensors in AMS.

2.2 Project Specific Aims

This objective was pursued by achieving three specific aims.

Aim 1: Define the information needs to support decision-making during routine operations;

[3] The topics of underground fire detection and the use of sensor-based networks to detect fires is well researched and practiced. Moreover, specific requirements for their use is prescribed in the federal regulations. As such, this project did not consider sensor-location strategies for fire detection.

Aim 2: Define the salient characteristics of monitoring systems that could provide the information so identified;
Aim 3: Utilize the findings to prepare practical, "how-to" guidance for mine personnel.

3.0 Research Approach

Scenarios incorporating specific events that can lead to potentially hazardous conditions are referred to as *event scenarios* in this report. The event scenarios identified for the purposes of this research are described in Section 4.1. Once the event scenarios were selected, the next step was to identify the information elements (i.e., sensor inputs) required in the decision-making process to confirm the existence of a developing and potentially hazardous condition. These sensor inputs are also presented in Section 4.1.

The foregoing work defined sensor inputs but did not establish the location of sensors nor the sensitivity required to detect incipient problems. The development of a strategy to locate sensors was carried out by examining maps from mines of differing size and complexity and identifying the locations of sensors to detect the event scenarios. This exercise led to a generalized strategy for choosing sensor locations, which is presented in Section 4.1. Determining the appropriateness of the locations and the sensitivity to event scenarios was investigated using ventilation models and computer simulations. The ventilation models were constructed using mine maps and ventilation surveys from operating mines. The models, simulations, and results are presented in Section 4.2.

Details on an in-mine validation effort are provided in Section 4.3. An in-mine data collection plan was developed to validate the proposed sensor-location strategy and the overall efficacy of the recommendations developed in this work. A cooperating mine with an extensive AMS was identified, and a conceptual design for a data capture system was completed. This system would allow the continuous flow of monitored data to be captured and stored without interfering with the mine's use of the AMS. The ensuing database, representing several months of monitoring experience, combined with operational details at the mine level, would provide the information needed to exercise and validate the strategy for locating sensors. Unfortunately, a sequence of external events that could not have been anticipated resulted in the removal of AMS from U.S. underground coal mines. This created significant challenges in this project, and the efforts to first resolve and then work around this issue consumed significant time and resources. Ultimately, in-mine experiments were conducted to validate the location strategy.

Finally, practical recommendations for the placement of sensors with the proposed location strategy, based on the results of the computer simulations and the in-mine validation, are summarized in Section 6.0. Notably, the use of pressure sensors is proposed in lieu of air velocity sensors. The rationale for this recommendation is described in Section 4.1, and the use of pressure sensors is shown to be efficacious in Section 4.3.

4.0 Research Findings and Accomplishments

4.1 Information Needs

Proper ventilation is critical for the safe and productive operation of a mine. Accordingly, operations personnel are keenly interested in ensuring adequate airflow to maintain methane concentrations well below the threshold requiring the removal of power from equipment. The

personnel also need to ensure that dust and other toxic or noxious materials remain below established thresholds, and that airflows exceed the statutory minimums.

The baseline condition for these needs is a mine ventilation system that has been correctly engineered and which has an MSHA approved ventilation plan. As mining progresses, changes in extent and complexity occur in the system. The demands for air on the working sections may change, leakage may increase, and aircourse resistance may shift. With the passage of time, ground conditions or gas liberation may vary. Bleeder systems may become larger and more complex, and so on. The net result is that the actual ventilation throughout the mine will be different from the designs' original predictions, and perhaps different from the conditions established in the ventilation plan. Of course, some changes should be identified from measurements taken at the evaluation points in the approved ventilation plan, but this is not a certainty. Moreover, miners on one section may change their regulator setting to get more air to their working faces; in so doing, they may not consider or understand the effect that this change could have on other parts of the mine.

Understanding and then managing these deviations from the design or expected values of ventilation parameters presents a constant challenge to mining personnel. It is important to distinguish short-term perturbations from longer-term trends. It also is critical to know whether a particular change is an indicator of a potentially serious situation that has developed or is developing.

The root causes of most deviations are well known by mining personnel. They include leakages that are larger or smaller than expected, increased aircourse resistance from deteriorating ground conditions or water accumulations, accidental or deliberate changes to ventilation controls, and equipment movement in airways, among others. Combinations of these factors as well as changes in barometric pressure cause deviations between the intended operation of the system and the actual performance.

The challenge for the mine operator, as just outlined, is to know which changes are indicative of unexpected or undesirable deviations. One goal in this research is to define the sensor-based information that would be needed to inform the mine operator's decision to do nothing and wait, to investigate further, or to take a more immediate corrective action.

4.1.1 Event Scenarios

The first step toward defining information needs was to query practicing professionals in operations, engineering, and enforcement positions to investigate the following questions:

- What are they looking for as they try to prevent ventilation problems that could affect production or safety?
- Which parameters receive the most attention and why?

The answers to these questions will reveal opportunities for sensors to meet information needs that are strongly aligned with safety concerns. To this end, project personnel began with in-person discussions with 23 mining personnel working in 12 different mines, and with three MSHA inspectors. This initial effort used a convenience sample across small, medium, and large mines located in the East, Midwest, and Western coal fields. Along with the questions indicated above, other discussion topics included questions on the potential value of AMS to help them complete

their work more effectively. The uniformity of the responses was so high that no additional sampling was deemed necessary.

As expected, all interviewees identified their focus as searching for signs of meaningful reductions in airflow or increases in methane, both of which could result in a production delay or a safety hazard. All started their day by looking at the barometric pressure and listening to the weather forecast to anticipate increased concentrations of methane resulting from falling atmospheric pressure[4]. All stressed the importance of looking at the fan charts to detect an increase in mine resistance, as indicated by a change in head and quantity at the fan. Most had an interest in the methane concentration at the main fan, and particularly any changes. Finally, there was unanimity in the measurement of airflow at key locations to detect significant changes. The only difference in opinion that emerged from these discussions concerned the amount of change that would constitute a *significant change*, i.e., a change that would catch their attention. The responses, in descending order of frequency, were:

- Air changes greater than 9000 cfm
- Air changes greater than 25% of the expected value
- Air changes greater than 10% of the expected value

These responses are predictable. The most common response was likely based on the 30 CFR 75.324, which considers a change of more than 9000 cfm to a section to be an intentional change requiring specific actions including removal of power and withdrawal of miners from the affected area. The percentage changes reflect the width of error band around the mean value, which is required to minimize type II errors (i.e., false positives). Personnel with some experience with sensors favored the larger error band of 25%. An appropriate magnitude for a *significant change* will be addressed later in this report, but regardless of the magnitude of the change, the underlying causes of the change are of interest.

Of particular interest here are causes that are not catastrophic in nature, likely to occur over time and go unnoticed, and/or the result of deliberate actions taken by mine personnel. It is likely that catastrophic changes will be noticed quickly, and attention will be focused on addressing the underlying problems. In contrast, changes that occur gradually and develop over time are more likely to go undetected. While these may ultimately present a hazard in their own right, the somewhat compromised state of ventilation may also leave the system vulnerable to other stressors. Similarly, deliberate actions by miners during a shift, such as changing a regulator or opening a door to direct more air to a working section, could create problems in other parts of the mine or leave other parts vulnerable. The system-wide impact of these intentional and likely unauthorized changes may not be apparent. As such, the detection of these changes is of interest in this project. Notwithstanding, the proposed sensor location strategy will also be able to detect catastrophic changes.

The following *event scenarios* have been identified:

- A gradual increase in aircourse resistance, most often resulting from a reduction in the cross-sectional area of the aircourse caused by:
    - an accumulation of water
    - a floor heave
    - a partial failure of the roof or rib

[4]

- A gradual increase in aircourse resistance after the development of new mine workings in excess of the original design capacity of the ventilation system
- Unauthorized or otherwise inappropriate changes to a ventilation control such as:
    - a change to a regulator to provide additional air on a production face
    - a door being propped open or left open to obtain additional air in a part of the mine.
- Excess leakage caused by
    - one or more stoppings being damaged or removed
    - overcast degradation
    - a door being propped open or left open
- Loss of pressure on the active longwall gob, allowing methane migration onto the face resulting from
    - change to the ratio of air flow at the t-split
    - inadequate airflow across the longwall face
- Leakage from sealed areas into active workings as a result of
    - leakage from seals.

Given these event scenarios, the next step is to identify the sensor inputs needed to support decision-making around these events, which is discussed in the next section.

4.1.2 Sensor Inputs

Identifying sensor inputs to serve as sentinels for the event scenarios defined in Section 2.1 is straightforward. Airflow, or a surrogate of airflow such as air velocity or pressure, is required to diagnose each of the event scenarios, except for the last one in the list, which requires knowledge of methane concentration.[5]

Airflow in underground mines has been measured manually using a variety of methods to determine the air velocity,[6] which is then multiplied by the cross-sectional area of the aircourse to obtain the volume flowrate. Vane anemometers remain a common means of measuring air velocity, and it was only natural that the air velocity sensors developed for the first mine monitoring systems were adapted from the classical vane anemometer. These devices had all of the drawbacks of vane anemometers plus a new one: float dust accumulated on the vanes, introducing significant measurement error. The moving vanes were eventually replaced with a sensor that has no moving parts, known as an ultrasonic air velocity sensor. These devices eliminated the problems associated with the ball-bearing-mounted vanes that could be easily damaged. Ultrasonic sensors are accurate and mine-worthy. Unfortunately, they do not overcome three fundamental shortcomings attendant on air velocity measurement: sensitivity to local perturbations in the airstream, sensitivity to small changes in the spatial orientation of the sensor, and errors associated with a single-point measurement. Each method is briefly described below, and then an alternative to the traditional means of determined flowrate is proposed (Kohler 1986, Kohler and Thimons, 1987).

[5] The strategic location of sensors to detect combustion is a well-known practice based on Bureau of Mines and NIOSH research, as stated earlier in this report. Accordingly, combustion events and the attendant sensor placement were not revisited in this project. The mine seal methane leakage is not the focus of this project because the sealed region is typically not considered for the mine ventilation simulations.

[6] The term *air velocity* is commonly used in the literature and in practice rather than *air speed*, even though it is only the magnitude of the air velocity that is being described. The term *air velocity* will be used in this report to be consistent with practice.

Single-Point Measurement. The air velocity in the cross section of the aircourse varies considerably (50% or more). Generally, the highest speed occurs near the center of the cross section and the lowest speeds are found near the walls of the aircourse. Multi-point traverses can be used during the initial sensor installation to obtain a more accurate average speed, and this can be used to compute a correction factor to relate the measured speed at the sensor to the average value. Unfortunately, if the flow through the opening increases or decreases, the isovels will change and the previously computed correction factor will be incorrect.

Spatial Orientation*.* Initially, the sensor will be installed so that the measurement head is orthogonal to the direction of airflow. A change in this angle, either yaw or pitch, of more than a few degrees will result in a noticeable and potentially significant change in the reported air velocity. Such changes are not uncommon when the mounting arrangement for the sensor is disturbed inadvertently or deliberately.

Local Perturbations*.* The cross-sectional velocity profile (i.e., the isovels) are sensitive to activity upstream of the sensor by as much as ten diameters or downstream by three diameters. Equipment and personnel movement will cause changes in the measured velocity even though the flowrate may remain unchanged.

The effect of these three confounders is a very "noisy" signal, i.e., point-to-point fluctuations in the measured air velocity. Fluctuations of ±10% are common and ±15% is not uncommon.

Alarm values are normally set for each sensor in the AMS software to communicate a sensor value that has crossed a threshold. Air speed sensors, which typically present with this level of "noise," require a dead band of 20% or more around the trigger value to prevent false alarms. The concern is that important changes inside of this large dead band could go unnoticed. In the early stages of the project, ultrasonic air velocity sensors were selected for the in-mine data collection component of this research. After the first in-mine experience and additional investigation, the decision was made to utilize pressure transducers instead. By knowing the area of a regulator opening and the pressure across the regulator, the volumetric airflow rate can be computed accurately. More generally, knowing the pressure at different points in the mine ventilation network facilitates the detection and analysis of problems that can lead to disruptions in the ventilation system.

The mine ventilation Square Law is the single most important relationship for mine ventilation planning and ventilation interruption diagnosis. The relationship between frictional pressure drop and resistance can be expressed as (McPherson, 1993):

$$p = RQ^2 \text{ or } \quad P_{ij} = \Delta p = RQ^2 = RA^2v^2 \tag{4-1}$$

where P_{ij} is the differential pressure from position *i* to position *j*. The parameter R is the Atkinson's resistance of the airway.

The frictional pressure drop is jointly determined by airway resistance (R) and airflow quantity (Q). In essence, most ventilation disruptions are caused by aircourse resistance changes, which in turn change the airflow quantity and airflow distribution.

According to the Square Law Eq. (4-1), the frictional pressure drop (p) can be influenced by both R and Q. Because p is proportional to the square of Q, p is more sensitive than Q to changes in R;

therefore, *p* will be more sensitive to changes in *R* than the measured surrogate for Q, i.e., air velocity, *v*.

Ventilation interruption and failure are attributed to mine resistance modification, and therefore, it is important to detect these changes of the mine air course resistance. For this purpose, pressure monitoring is superior to velocity because it is more sensitive to small changes and is unaffected by the confounders that impact air velocity measurements, as described earlier in this section. Accordingly, the signal will be less noisy, and this eliminates the need for a large deadband around the trigger level for the sensed value.

A simple in-mine experiment was planned to compare the use of the traditional velocity and the pressure sensors as surrogates for airflow quantity, *Q*. A data acquisition system was constructed using an off-the-shelf data logger (MCR-4V). The data logger was mounted inside of the outstation provided by Matrix Team. The air velocity sensor, also provided by Matrix Team, was connected to the outstation. The outstation required a 110V power source. The outstation and air velocity sensor are shown in Figure 4-1.

Another MCR-4V data logger was mounted in a Pelican box along with a small battery to power the data logger. The power supply for the pressure transducers was also housed in this box along with the interface electronics. Two Setra pressure sensors were mounted to this Pelican box[7]. This assembly was not considered intrinsically safe, and accordingly was located in fresh air. The regulators being monitored were in return air, which did not present a problem because Tygon tubing was used to connect the transducers to the atmosphere on either side of the regulator. The pressure recording instrumentation is shown in Figure 4-2. Additional detail on the data acquisition system and the Setra pressure transducer are presented in Appendix I. The collected data was stored on an SD card and extracted using software provided by the manufacturer of the data logger.

Both velocity and pressure instruments were installed in the main of our partner underground coal mine. Both instrument packages were recording the same airflow. There is a regulator nearby this monitoring location which it was the targeted sensor location to monitor the differential pressure variation as discussed in the *Section 4.1.4 General Strategy for Sensor Location*.

The air velocity sensor and the associated outstation were placed in fresh air near a 110V source. The velocity sensor package shown in Figure 4-3 was installed in the intake airway of the main marked as blue dot. The pressure sensor instrument shown in Figure 4-2 was installed at the fresh air marked red dot in Figure 4-3. Tygon tubing was used to extend the monitoring points across a regulator between the intake and return and the monitoring points are illustrated as green dots. Differential pressure was computed by the barometric pressure readings from two green dots' positions. This is illustrated in Figure 4-3.

[7] A differential pressure transducer with the required sensitivity was not readily available at the time the instrument package was being designed. Instead, two atmospheric pressure transducers were used and the differential pressure was computed from the collected data.

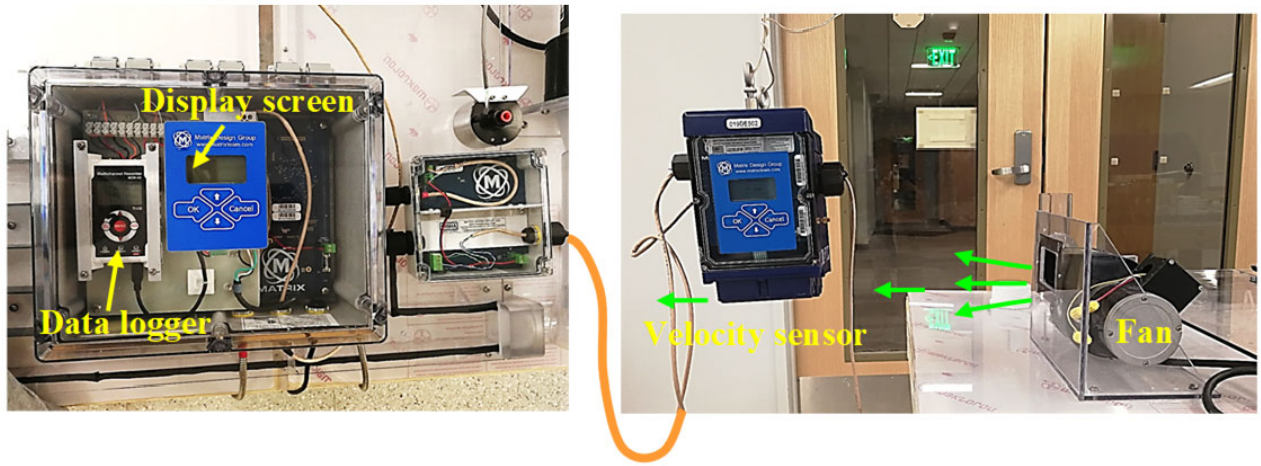

Figure 4-1. Velocity sensor with embedded data logger in the outstation.
Note: The equipment is shown in the laboratory.

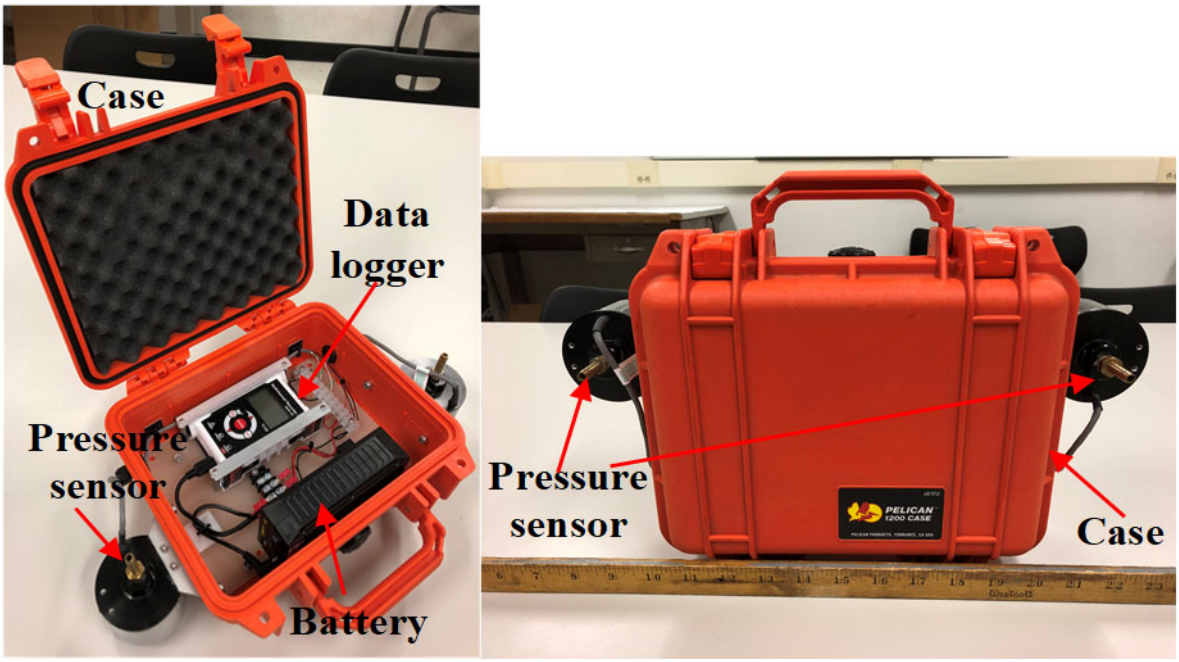

Figure 4-2. Differential pressure sensor with embedded data logger.

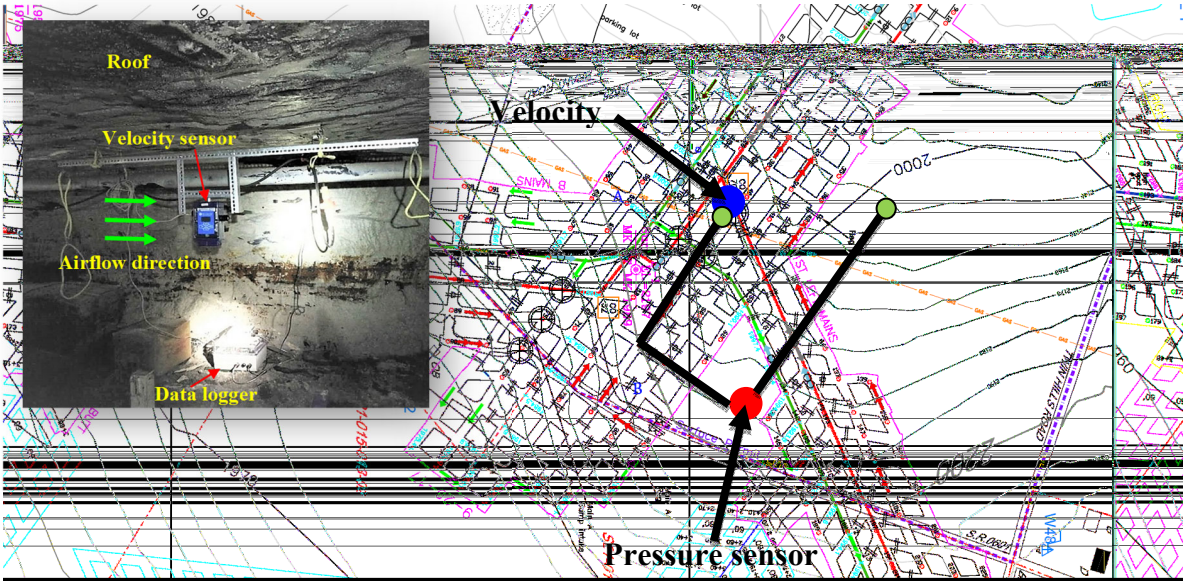

Figure 4-3. In-mine sensor installation and sensor positions.

Recordings were taken over a two-week period. Data from the first seven-day period is shown in Figure 4-4, which is used to illustrate the advantages of using pressure rather than velocity as a surrogate for *Q*.

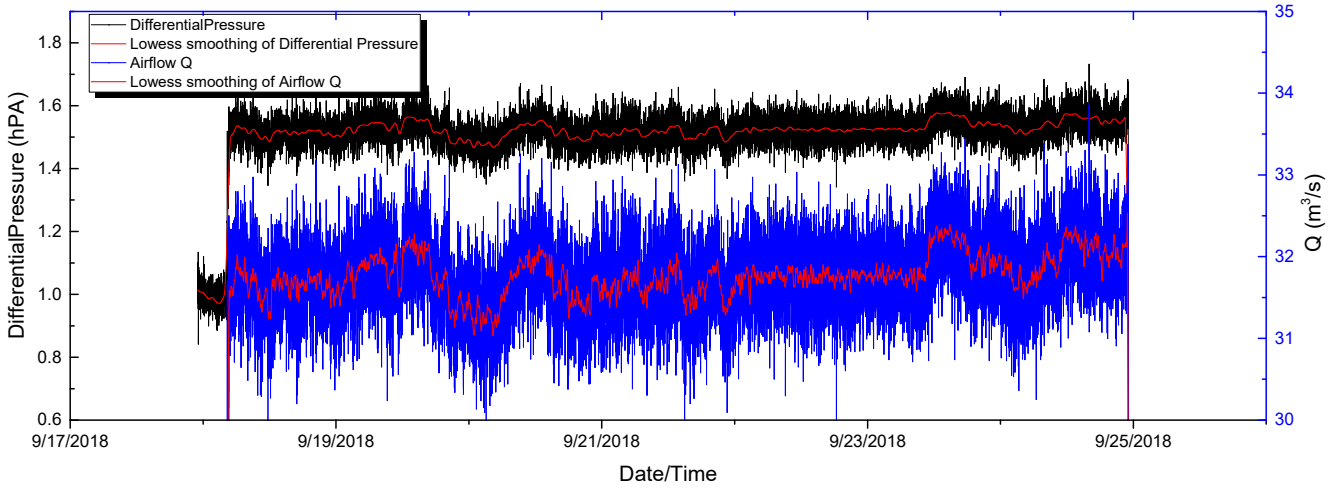

Figure 4-4. Comparison of velocity and pressure as surrogates of air quantity.

In Figure 4-4, the black trace is recorded pressure and the blue trace is recorded airflow. The estimated airflow was computed by the measured air velocity (through ultrasonic velocity sensor) times the fixed cross-sectional area. There were no ventilation interruptions during this seven-day period. Two important observations from the figure are that both surrogates move in unison, but pressure is far more stable (i.e., less noisy) than velocity. This of course is a compelling reason to use pressure rather than velocity as a surrogate for quantity. A smoothing algorithm (Lowess) was used on each signal, and the result is shown in red trace. Although this removes some of the apparently random changes in the signal for velocity, it does not change the apparent superiority of pressure. Figure 4-5 is the statistical analysis of the directly measured data presented in Figure 4-4. To directly compare airflow and differential pressure data, the raw data were initially processed

through the Lowess algorithm and then both airflow and differential pressure data were normalized against their average values for the whole monitoring duration (7 days for this case). The mean and standard deviations demonstrated in Figure 4-5 is the statistical analysis of normalized airflow and different pressure data. Y-axis represents the counts of numbers within each column bin. The narrow-shaped pressure distribution with a smaller standard deviator suggests that the differential pressure data is more stable compared to widely distributed airflow data. When the mean of normalized data is approaching to one, it represents that the original monitored data keep somewhat constant at a single flat value which is desirable. From Figure 4-5, it is concluded that the different pressure data are more stable and reliable compared to the airflow monitored data which is a justification of the pressure monitoring system. Using the different pressure monitoring data, it allows the operator to further tightening of the deadband around any alarm level for the active monitoring system.

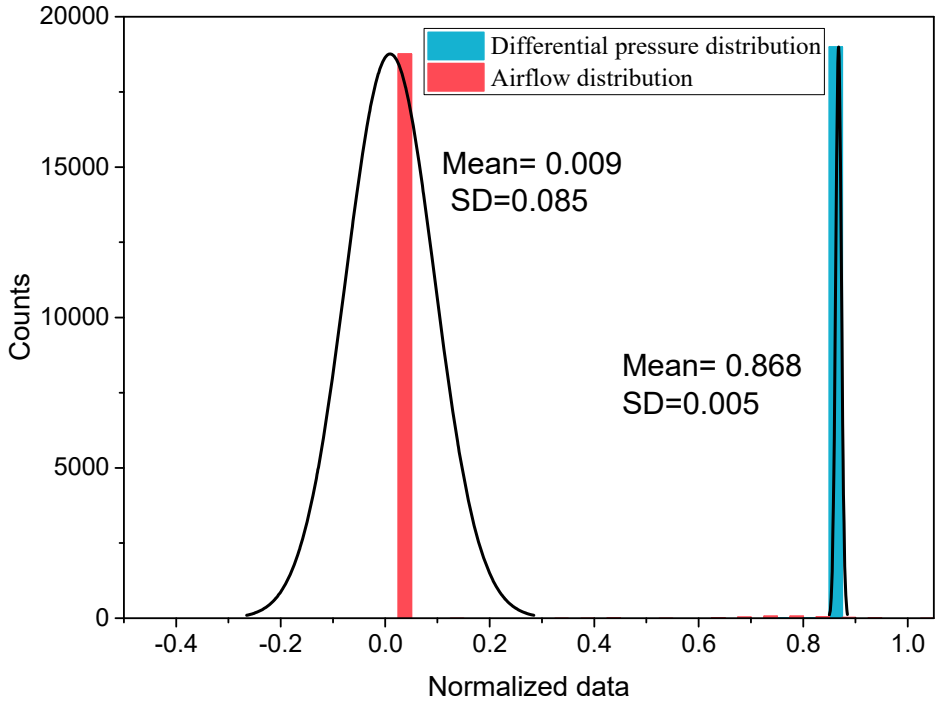

Figure 4-5. Mean and standard deviation for the waveforms shown in Figure 4-4.

The use of pressure transducers, whether a differential transducer or two pressure transducers, allows for yet another practical benefit. The transducer need not be placed at the spot where the pressure must be measured. Plastic tubing can be run for a few inches or hundreds of feet to connect the transducer with the atmosphere being measured. This offers certain economies in terms of intrinsic-safety or permissibility requirements, while also enabling the transducer and the connection to the mine's data network to be located out of harm's way. Commercial pressure transducers with the required level of sensitivity are readily available at a reasonable cost. The transducers used in this research are described in Appendix I. The use of pressure transducers in a mine-wide system for routine and post-accident application is presented in Section 4.3 of this final report.

Throughout the remainder of this report, it is assumed that the airflow will be computed using a pressure rather than an air velocity measurement. Measurement of the methane concentration can

be carried out using traditional methane monitors, and these sensors are not discussed further. Having justified the choice of sensor type, the next step is to address the location of these sensors to achieve the stated goal of this project.

4.1.3 Sensor Location Strategy

A long-standing practice in atmospheric monitoring has been to co-locate airflow, methane, and carbon monoxide sensors (Cohen, 1987). This practice was an electronic convenience in the early days of AMS by economizing on supervisory control, data acquisition, and communication circuits. These efficiencies are no longer concerns with today's technology, which is inexpensive, small, and consumes minimal power. Nonetheless, the practice of co-location is still viewed as "the way it's done." Such an approach needlessly increases the initial cost of the system and the ongoing cost to calibrate and maintain sensors that may be contributing little useful information to decision-making. The location of carbon monoxide sensors should be based on the need for early-combustion detection, whereas the location of airflow and methane sensors should follow from the logical end-use of the acquired information. Sometimes logic will dictate that all three be co-located, but this is often unnecessary. Why is a sensor being placed at a location? What data will the sensor provide to inform operations? These questions are fundamental to the location strategy developed in this research. The event scenarios identified in this project rely almost entirely on knowing airflows, and methane is only required in one event scenario.

The goal of this project, as previously explained, is to deploy as few sensors as possible, while maximizing the value of the information provided by those sensors. The task at hand is therefore to formulate a strategy to locate sensors that would inform decisions related to the event scenarios defined in Section 4.1.1. It is useful to think of such sensors as *sentinels*, because they are being located to provide an early detection of developing problems in the mine ventilation system.

Concurrently, a distinction must be made between sensors that will detect a problem versus additional sensors that will help to locate the specific source of the problem. An AMS with the ability not only to detect the development of a problem but also to pinpoint the location or source of the problem would seem to be ideal. The tradeoff, however, is in the number of sensors required, and significantly more sensors would be needed to improve location accuracy. Certainly, adding more sensors with a defined purpose cannot be discouraged. Nonetheless, the current operational reality is such that additional sensors create an additional workload and expense that is not offset by the value provided by those sensors. This may not be the case if, in the future, AMS applications of artificial intelligence are developed to automate the interpretation and decision-making associated with these sensors. Currently, the most immediate need is to define a smaller set of sensors to detect developing problems. The expectation is that a mining professional would then investigate to determine the exact location and cause of the developing problem.

The methodology employed to develop a generalizable location strategy was straightforward. Mine maps were acquired for several mines with differing characteristics. Initially, the plan was to categorize the mines by size into three categories: small, medium, and large. The initial criteria for defining size were the number of working sections and the presence of one or more longwall sections. After further discussion and review of the maps, two categories were defined: mines with a longwall and mines without a longwall. The next step was to identify sensor locations in each mine. The locations were chosen so that each of the event scenarios could be detected. Once completed, the set of sensors was examined to identify redundancies or gaps in sensor locations. General guidance to locate the sensors was formulated from this assessment.

This proposed location strategy is presented in Section 4.1.4. First, the following subsection summarizes the terms used to identify sensor locations in coal mines.

4.1.3.1 Mine layout terminology and definitions

The guidance given for sensor locations utilizes common terms to describe locations. A brief summary of a coal mine layout is given here to prevent any ambiguity in the use of these common terms.

Underground coal mines begin at an access point or portal, which may be: a drift from a face-up in the side of a box cut or hillside where the coal seam is exposed; a slope driven from the surface and through the overburden, to the coal seam; or a shaft driven from the surface down to the coal seam. Typically, a main fan is located near the portal because the access to the mine usually includes a major aircourse for the mine's ventilation system.

The mine's major development begins at the pit mouth, slope bottom, or shaft bottom. *Main entries* or *mains,* which may consist of nine or so individual entries, open up the deposit for exploitation and serve as the major intake and return aircourses. The major materials handling systems for personnel, supplies, and coal, the electrical power distribution system, and water lines are located within these mains. The *entries* carrying fresh air are designated as *intake aircourses* or *intakes*, and those aircourses that carry air that has been contaminated with dust and gas are known as *return aircourses* or *returns*.

In smaller mines with only one or two *room and pillar sections*, *production panels* may be driven directly off of the *mains*, and each *panel* would have one active *working section*. Ventilation, materials handling, and power to the *working section* are provided from the mains. The airflow to the working section is controlled using a *regulator* that is located in the re*turn aircourse*, i.e., the return entry of the production panel. The effective size of the regulator opening changes the resistance of the aircourse, thereby controlling the quantity of air flowing through the section.

In mines with only a few continuous mining units, but a larger deposit, it may be necessary to drive *submains* off of the *mains*, and then *production panels* off of the submains. In many cases, the *submains* carry air and services to multiple production panels, and as such will require five or so entries.

The *room and pillar production panels* typically consist of three-to-nine entries and often have a length of 2000 to 5000 ft.

Those mines using *longwall mining* define their *longwall panels* by driving two three-entry gate roads, on the *headgate* and the *tailgate* side of the panel. Fewer than three entries will rarely be used in the U.S. The width of the longwall panel (i.e., the face) can be up to approximately 1600', while the panel length usually exceeds 12,500' and may approach 25,000'. Usually, the large size of the deposit in a longwall mine dictates that the longwall panels will be developed off of *submains*. Five *longwall panels* typically define a *district*, and the district will be sealed from the remainder of the mine when the panels have been mined.

Bleeder entries, or *bleeders*, are developed around the periphery of the panels to carry away any methane that is liberated from the mined-out areas. In longwall mines, it is likely that each district will have a *bleeder-shaft fan* to assist in the removal of methane from the gob. Typically, a shaft of at least 6' in diameter is constructed to connect the bleeder to the surface, and surface-mounted

exhaust fan is installed. The air will split at the tailgate-end of the face, with a fraction going to the bleeders and the remainder going into the tailgate return. This point is often known as the *T-split*.

4.1.4 General Strategy for Sensor Location

The goal of the proposed strategy is to strike a balance between the number of sensors required and the value of the information acquired by those sensors. In essence, this strategy aims to achieve the smallest possible set of sensors to serve as early-warning indicators (i.e., sentinels) of developing problems. As explained above, pinpointing the exact location of the problem is not a high priority. Nonetheless, some locations that would be primarily useful for specifying the source are included but are clearly identified for this purpose. There may be instances where additional sensors are needed to address certain concerns specific to the mine, e.g., a mine on a spot-inspection order for excessive methane under Section 103(i) of the Act.

Adequate airflow on the working sections is critical, and a change from the expected value on the sections is cause for investigation. Monitoring for a change in the quantity of air to a room and pillar section can be detected at a single location, at the *section regulator*. As such, the section regulator is a critical place to monitor. Historically, air quantity has been determined by measuring air velocity, but this has been problematic, as explained in Section 4.1.2. Rather than measuring air velocity, as is traditionally done, it is recommended that the pressure be monitored across the section regulator.[8] Monitoring of methane at this location is not advised. If adequate air is provided under the ventilation plan, there should be no need to monitor methane independently. If a gassy pocket is encountered during mining, the equipment will be de-energized automatically or the increase in methane concentration will be detected during routine gas checks. In the very unusual context of a mine culture wherein the machine-mounted monitor would be disabled, or routine gas checks neglected, there would be a risk that a serious problem could develop unnoticed. However, this risk will not be necessarily mitigated by using a methane monitor outby the section regulator, simply because it is likely that it would be disconnected as well. Therefore, the recommendation is to monitor air quantity, i.e., the pressure across the regulator, but not methane at the section regulator.

Providing sentinels for a longwall section requires a few more monitored points than for continuous miner room and pillar sections. The pressure across the regulator in the return entry at the mouth of the section is an important location, as it was for room and pillar sections.

The t-split shown in Figure 4-6 is a critical location. It is essential that the pressure at the tailgate with respect to the pressure in the bleeder entry (#2 entry in Figure 4-6) be maintained to ensure that there is adequate airflow from the tailgate to the bleeder entry. Therefore, it is important to monitor the pressure between the tailgate and an outby point in the tailgate entry, which is being used as a bleeder. The pressure transducer should be located at the tailgate and a rubber tube should be run outby the face in the #3 entry (tailgate return) and terminated by placing it through a hole in the stopping separating the #3 (tailgate return) from the #2 (bleeder). It is recommended that this termination point be three to five stoppings outby the tailgate to minimize the number of times that it must be moved. Further, a small pipe (< ½”) should be installed in these stoppings when they are constructed. This will facilitate the movement of the rubber tube and ensure that no one has to go into the #2 entry to place or remove the tube as the longwall face retreats. Once the tailgate approaches this stopping, it will be necessary to relocate the tube to an outby stopping.

[8] The advantages of measuring differential pressure rather than air velocity are shown in Section 4.3, which describes the in-mine validation performed for this research.

There are certainly other regulators and points that could be monitored for the longwall, but from a safety perspective and consistent with the goal of identifying only critical sentinels, monitoring at the t-split is the key sentinel. Notwithstanding, monitoring the pressure drop across the tailgate regulator, labeled in Figure 4-6, could serve an important sentinel function. If a partial obstruction were to develop in the tailgate return entry, some distance outby the tailgate, it may not be readily detected at the t-split. Given the relative ease of establishing a sentinel at this regulator, it is recommended that it be added.

There are variations on the ventilation design for longwalls, given unique conditions in certain mines. Regardless of these variations, it is critical to monitor the t-split to ensure that conditions there agree with design or plan values. Depending on unique circumstances at a mine, it may be useful to add an additional sentinel.

The foregoing discussion has focused on capturing air quantity, i.e., pressure, as a surrogate for quantity. There is little need to monitor methane to achieve the desired early-warning functionality. In most cases, detecting disturbances to the flow will allow corrective action well before methane levels begin to rise. One notable exception is locations immediately outby points where sealed areas are adjacent to the submain or main return aircourses. These locations should be monitored for methane to detect the rare event in which methane leaks through the seals into the active mine workings.

Finally, the total head and methane concentration at the surface fan(s) can serve as sentinels and, as such, should be monitored. Other potential sentinels at the fan would include CO. Most mines already monitor these parameters at their fans.

The sensors and locations to serve as sentinels for the detection of developing and potentially hazardous conditions have been described in this section. Many additional locations could be added to aid in locating the source of a problem. Sensors at many of the evaluation points identified in the mine's ventilation plan would be helpful, but not essential, to alert mine personnel to a potential problem that they should investigate.

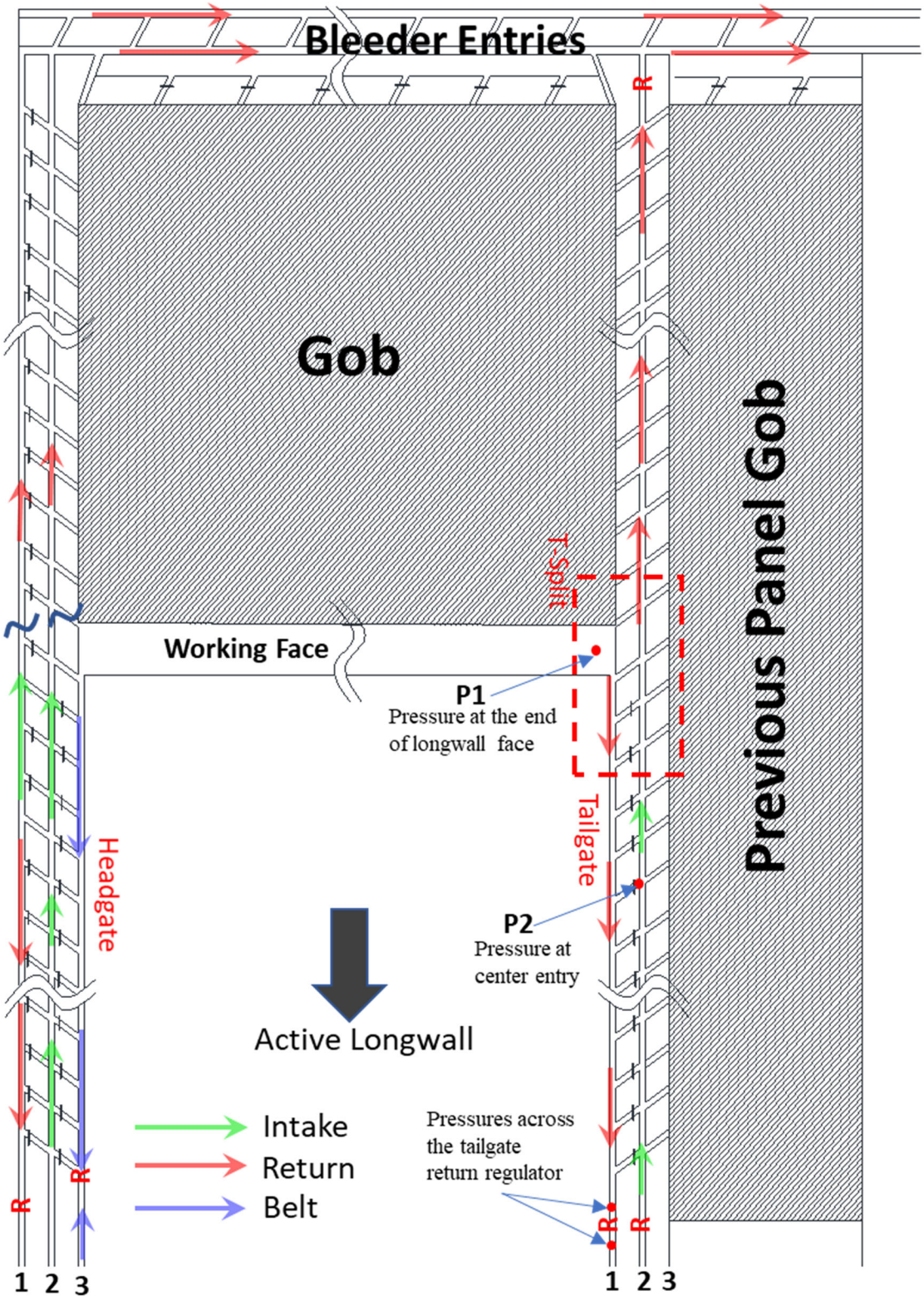

Figure 4-6. Placement of the pressure transducer and monitoring points to serve as a sentinel for the t-split.

4.1.5 Summary of Information Needed

Conditions that may compromise the mine ventilation system, which have been designated as *event scenarios*, have been identified in this section. A strategy for placing sensors to facilitate the early detection of these event scenarios has been presented. These sensors, or *sentinels*, were selected to minimize the total number of sensors by including only those that provide essential information for detecting potentially hazardous conditions. This set of sensors will not necessarily define the specific location of the problem and doing so will require human intervention. The efficacy of this strategy was tested using computer simulation. The details of these simulations and the findings are presented in Section 4.2. An in-mine validation effort was also completed, and this is described in Section 4.3.

4.2 Modeling and Simulation Studies

The purpose of the work described in this section was to determine the extent to which the event scenarios could be detected by sensors that were placed in the mine according to the proposed location strategy. As a first step, a map and the *p-Q* survey data set was obtained for a small and a large mine. The small mine was representative of the one-, two-, and three-unit mines commonly found in the U.S. The large mine was representative of mines with one or two longwalls and the associated continuous mining units.

The next step was to model the event scenarios for a range of severity levels. For example, for the problem in which the aircourse resistance increases, a full range of obstructions from very slight to full were modeled. Concurrently, the mine's ventilation network was built using the mine map and *the p-Q* survey data. A series of simulations were then executed using the ICAMPS MineVent software. The simulations were designed to study the sensitivity of changes within each event scenario at various locations in the mine, and particularly at the locations being proposed for the placement of sentinels. This approach is illustrated in Figure 4-7.

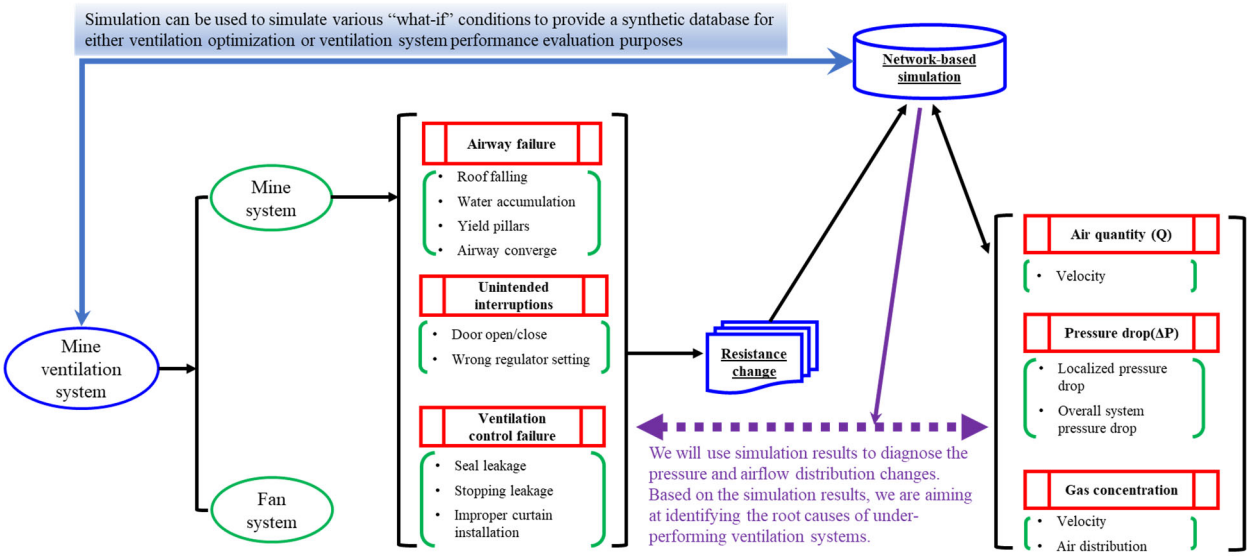

Figure 4-7. Illustration of the simulation approach used to investigate the ability of sensors in specific locations to detect developing problems.

A description of the modeling and the results of the simulations are presented in this section.

4.2.1 Network Model Establishment and Simulation

The Ohio Automation ICAMPS software package, which is based on the expanded Hardy Cross algorithm, was used in this research. ICAMPS-MineVent is an AutoCAD-based network drawing program in which the designated network nodes and branches can be mapped by using AutoCAD snap features on the basis of as-mined and/or projected timing maps. Mine ventilation network simulation typically starts with building the mine geometric structure network, which includes nodes and branches. In the network model, each branch is defined by a "*from*" and "*to*" junction number. It is a common practice to integrate parallel airways into a single branch.

After the geometric network is established, the input parameters defining the branches and the mine fan must be entered in order to execute the simulation. The branch information includes the type of each branch, e.g., fixed resistance or fixed/regulated airflow, and the branch resistance. The branch resistances can be specified in ICAMPS in the following ways: (1) directly as a fixed value defined by the user; (2) as an estimate from the measured pressure drop (p) and airflow quantity (Q); or (3) from an implied friction factor (k), airway geometry, and an indication of shock losses through Atkinson's equation. The fan data for the simulation is entered by the user either as a fan curve or as a fan table with pressure and volume data provided by the fan manufacture.

In this study, two ventilation network models were established: one for the small room and pillar coal mine (hereinafter referred to as the "small mine") and the other for a large underground longwall operation (hereinafter referred to as the "large mine"). Both models were built based on p-Q ventilation survey data. The manufacturer-supplied fan curves were used for the simulations. The mine maps were used to establish the intake, return, belt, and leakage branches network for both mines. The resistance of each branch was estimated by inputting p-Q survey data for the mine. After the model was run, the results were compared to the survey. The branch parameters were adjusted until a satisfactory agreement between the model output and the survey data was achieved. This validated model was then used for the base case and the starting point for the simulations.

4.2.2 Branch Resistance Estimation and Modeling

The first event scenario of interest is the gradual increase in airway resistance, which may result from an accumulation of water in the airway or ground control events. Out of all scenarios, this is known to be the major and most common cause of mine ventilation disturbances. (MSHA, 2016). Regardless of the cause, the result is an increase in the resistance of that aircourse due to a reduction in the cross-sectional area and the roughness of the aircourse. Three common causes are illustrated in Figure 4-8.

To quantify the frictional pressure drop across an air branch, Atkinson's equation is introduced (McPherson, 1993):

$$p = kL\frac{O}{A}v^2 \tag{4-2}$$

where p is the pressure drop of an airway with length L, cross-sectional area A and perimeter O, v is air velocity, and k is the Atkinson friction factor.

Writing Atkinson's equation in the terms of airflow, $Q = vA$, results in the following:

$$P = kL\frac{O}{A^3}Q^2 \tag{4-3}$$

And, then combining the square law of mine ventilation, $P = RQ^2$, the airway resistance is expressed as:

$$R = kL\frac{O}{A^3} \tag{4-4}$$

For airways with a circular cross section:

$$O = \pi d, A = \pi(d/2)^2 \tag{4-5}$$

Therefore,

$$R \propto \frac{1}{d^5} \tag{4-6}$$

This proportionality can be rewritten as:

$$R \propto \frac{O}{A^{\frac{1}{2}}}\frac{1}{A^{\frac{5}{2}}} = SF\frac{1}{A^{\frac{5}{2}}} \tag{4-7}$$

where SF is the shape factor.

The shape factor is a constant for a given shape cross section. It has been proven that a circular airway will have a minimum possible shape factor at 3.5449 as estimated by:

$$SF(circle) = \frac{O}{A^{\frac{1}{2}}} = \frac{\pi d}{d\sqrt{\pi/4}} = 3.5449 \tag{4-8}$$

The shape factor for non-circular shapes will be greater than the value for the circular cross section. The shape factors for other shapes are generally normalized with respect to the circular airway through the relative shape factor, and this relative shape factor is defined as the ratio of the shape factor for the given geometry to the shape factor for the circular airway (3.5449). Relative shape factors deriving from several width-height rations for the rectangular airway considered in this study are listed in Table 4-1.

For rectangular airways, $O = 2(a + b)\ and\ A = ab$, where a and b are the length of horizontal and vertical side of rectangular airway.

$$R = kL\frac{2(a+b)}{(ab)^3} \tag{4-9}$$

The hydraulic diameter of rectangular can be expressed as:

$$d = \frac{ab}{2(a+b)} = \frac{a}{2\left(\frac{a}{b}+1\right)} \tag{4-10}$$

On this basis, the cross-sectional area reduction induced resistance change can be estimated, and these were shown in Table 4-1.

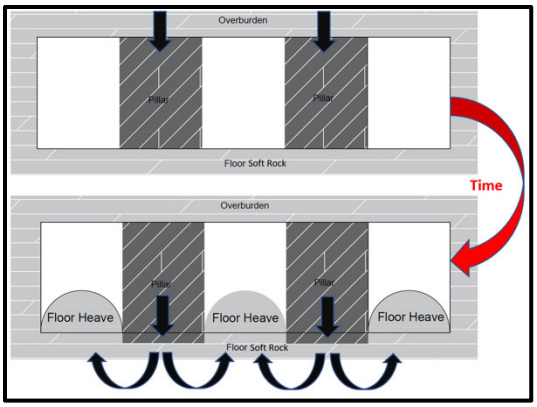

a. floor heave with soft mine floor

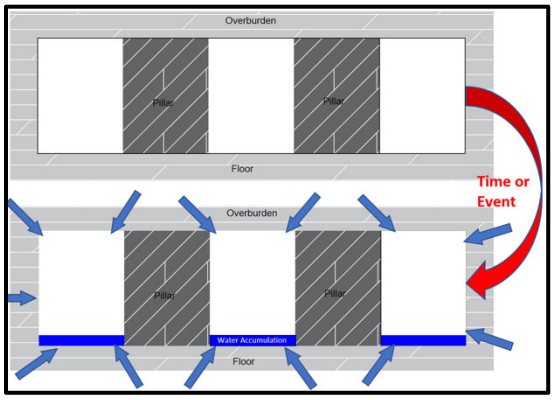

b. water accumulation

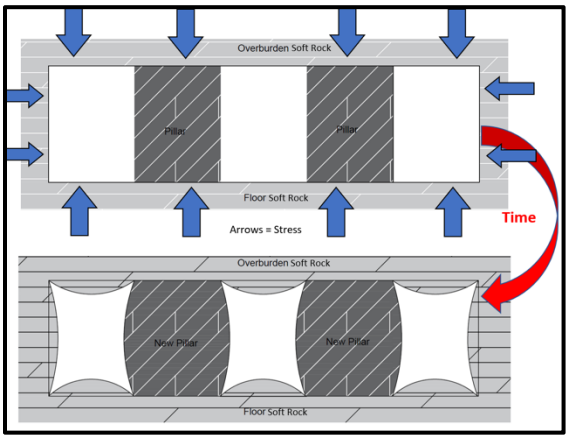

c. convergence of openings

Figure 4-8. Common causes of ventilation system disturbances.

4.2.3 Parallel-Airway resistance

In the modeling of coal mine room and pillar layouts, the *p*-*Q* survey is always simplified by considering several parallel airways with the same function as one airway branch and calculating the resistance based on parallel airway connection for its equivalent resistance as:

$$\frac{1}{\sqrt{R_t}} = \frac{1}{\sqrt{R_1}} + \frac{1}{\sqrt{R_2}} + \cdots + \frac{1}{\sqrt{R_n}} \quad (4\text{-}11)$$

where R_t is the total resistance of *n* parallel airways and R_i is the *i*th parallel airway.

Table 4-1. Resistance values for rectangular airways shown in Figure 4-8, with various width-height ratios.

Cross section shape	Width-height ratio	Relative shape factor	Cross section area	Resistance	Parallel airway	
					Single airway collapse	Double airway collapse
	a/b	$2(\frac{a}{b} + 1)/\sqrt{a/b}$	$1.5/(a/b)$	$R_e = C/d^{5}$	$R = 1/(\frac{1}{R_e} + 1 + 2/\sqrt{R_e})$	
Rectangular	1.5	1.15	A	R_e	$R_t = 0.25R$	$R_t = 0.25R$
Rectangular	1.75	1.17	0.86 A	1.61 R_e	1.25 R	1.61R_t
Rectangular	2	1.20	0.75 A	2.49 R_e	1.50 R	2.49 R_t
Rectangular	2.5	1.25	0.60 A	5.38 R_e	1.95 R	5.38 R_t
Rectangular	3	1.30	0.50 A	10.49 R_e	2.34 R	10.49 R_t
Rectangular	3.5	1.36	0.43 A	18.90 R_e	2.64 R	18.90 R_t
Rectangular	4	1.41	0.38 A	32.00 R_e	2.89 R	32.00 R_t
Rectangular	5	1.51	0.30 A	79.63 R_e	3.23 R	79.63 R_t
Rectangular	6	1.61	0.25 A	172.10 R_e	3.45 R	172.10 R_t
Rectangular	7	1.71	0.21 A	335.54 R_e	3.60 R	335.54 R_t
Rectangular	8	1.80	0.19 A	604.66 R_e	3.69 R	604.66 R_t
Rectangular	9	1.88	0.17 A	1024.00 R_e	3.76 R	1024.00 R_t
Rectangular	10	1.96	0.15 A	1649.16 R_e	3.81 R	1649.16 R_t

Note: a and b represent the length and width of rectangular airway; A and R_e are the initial cross-sectional area and initial unit length airway resistance; and R_t is the initial resistance of parallel airway system. All calculation formulas are from McPherson (1993).

The small mine case, described in the next section, has two parallel intake entries, two parallel belt entries, and one single entry serving as the return. As described above, a roof fall or entry convergence will reduce the area of the entry and increase the roughness of the inner surfaces, both of which will ultimately increase the resistance of the airway and change the airflow distribution. According to Equation (4-9), as the cross-sectional area decreases, the airway resistance increases. For parallel entries, the roof fall or entry convergence may occur within a single airway due to support failure or overburden stress compression. However, such an event may simultaneously affect both entries if, for example, the pillar between the two parallel entries is deformed, as conceptually illustrated in Figure 4-9(a)&(b). The estimation of resistance modifications should therefore be different for these two cases. Resistance change due to roof fall/airway convergence is evaluated in Table 4-1, where roof falling/airway convergence is divided into several subcases with various width-height ratios representing subtle, moderate, and severe roof fall cases.

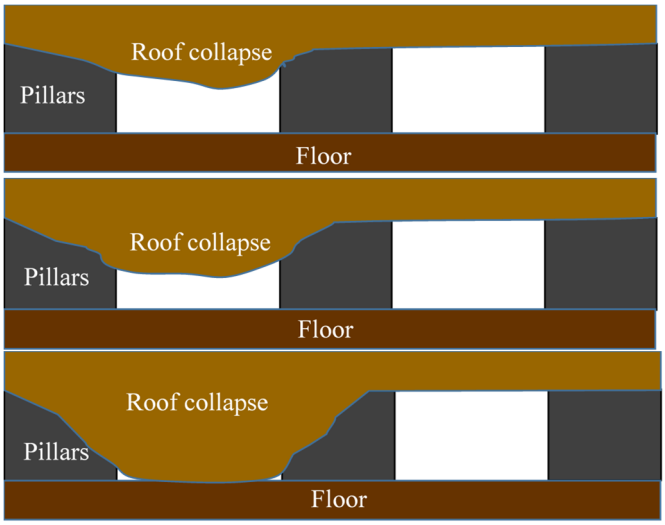

a. Single airway roof falling/deformation in a parallel system

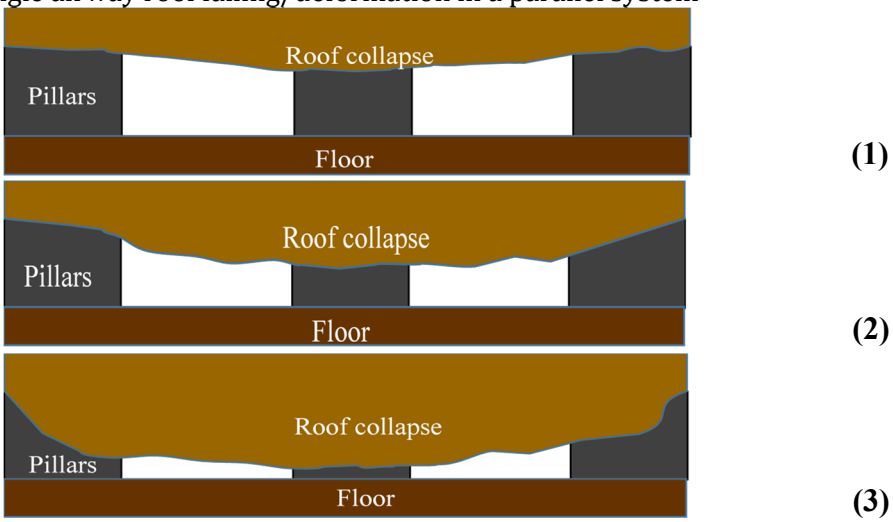

b. Coal pillar collapse-induced roof falling/deformation in a parallel airway system

Figure 4-9. Illustration of roof falling/roof convergence in parallel airways.

Figure 4-9(a) illustrates the single airway convergence cases that cause various perturbations on the initial ventilation system. The corresponding resistance change due to roof falling/deformation is listed in Table 4-1. In a parallel-airway system, if even one of the airways fully collapses, the total resistance is 4 times based on the parallel law ($R_t = 0.25R$). This incident can lead to the local pressure and velocity variations, but it is difficult to detect remotely because this type of incident may only slightly change the ventilation parameters in the overall mine system. In contrast, the roof falling/convergence caused by pillar collapse in a parallel airway system (Figure 4-9(b)) can lead to much larger changes in both pressure and airflow distributions in different regions of the whole ventilation system. The resistance calculation in Table 4-1 indicates that when the cross-sectional area is reduced to 50% of its original value, the resistance of this parallel-airway system will be 10 times its original value. When the cross-sectional area is reduced to 21% of its original value, the resistance can increase by as much as 336 times, which may cause a dramatic pressure or velocity change in the system. By installing the monitor at proper positions for sentinel purposes, the mine ventilation incidents can be detected in real time.

Based on these analyses, three values of resistance after the roof fall or other obstruction were chosen for the simulations to investigate how these changes influence the overall ventilation system. The three resistances are 32R, 335R and 1649R, which correspond approximately to a cross-sectional area reduction of 65%, 80%, and 85%.

4.2.4 Small Mine Simulation Studies

The small mine used in this study mined metallurgical coal in a 60" seam using two continuous mining sections. The mine map is shown in Figure 4-10(a) and the network used for the simulation is shown in Figure 4-10(b). Two roof fall incidents at different locations were numerically investigated using the validated ventilation model. The first roof fall incident is located at the intake heading of the submain. The second roof fall incident is located at the intake airways of the extended main. Both incidents are marked as red stars in Figure 4-10. To simulate different levels of severity of the roof fall, the branch resistance hypothetically becomes 32R, 335R, and 1649R, where R is the original branch resistance. These resistance values were selected based on the analytical resistance evolution for different levels of airway blockage. The detailed analyses were provided in the previous section.

The simulation was executed by manually increasing the designated branch resistance based on the values listed in Table 4-1, then running the simulation to achieve a new equilibrium. From the simulation results, both air quantity and pressure data at all branches and network nodes were reduced. The differential pressure for any two nodes can be calculated from the simulation results. According to the proposed sensor location strategy, the regulators were selected as monitoring points and two regulators were installed in the small mine. One is the regulator at the return of submain (marked M1) and another is installed near the portal between the return and belt airways (marked M2), as shown in Figure 4-10. For each roof fall incident, data reductions were run from the equilibrium simulation output, and the differential pressure across the regulators at M1 and M2 was estimated. The influence of each roof fall incident on the local and global ventilation system was analyzed by comparing the changes in differential pressure across different regulators in the mine.

Table 4-2. Results of differential pressure at different regulators with various roof fall pilots.

Roof fall pilots	Cross sectional area	Resistance	Differential pressure at M1	Differential pressure at M2
	A	R_e	0.44	0.57
Case1 the (Intake heading of the submain)	0.38A	32.00 R_e	0.31	0.59
	0.21A	335.54 R_e	0.07	0.62
	0.15A	1649.16 R_e	0.02	0.64
Case 2 (Intake of the extended main)	0.38A	32.00 R_e	0.54	0.55
	0.21A	335.54 R_e	0.67	0.49
	0.15A	1649.16 R_e	0.71	0.46

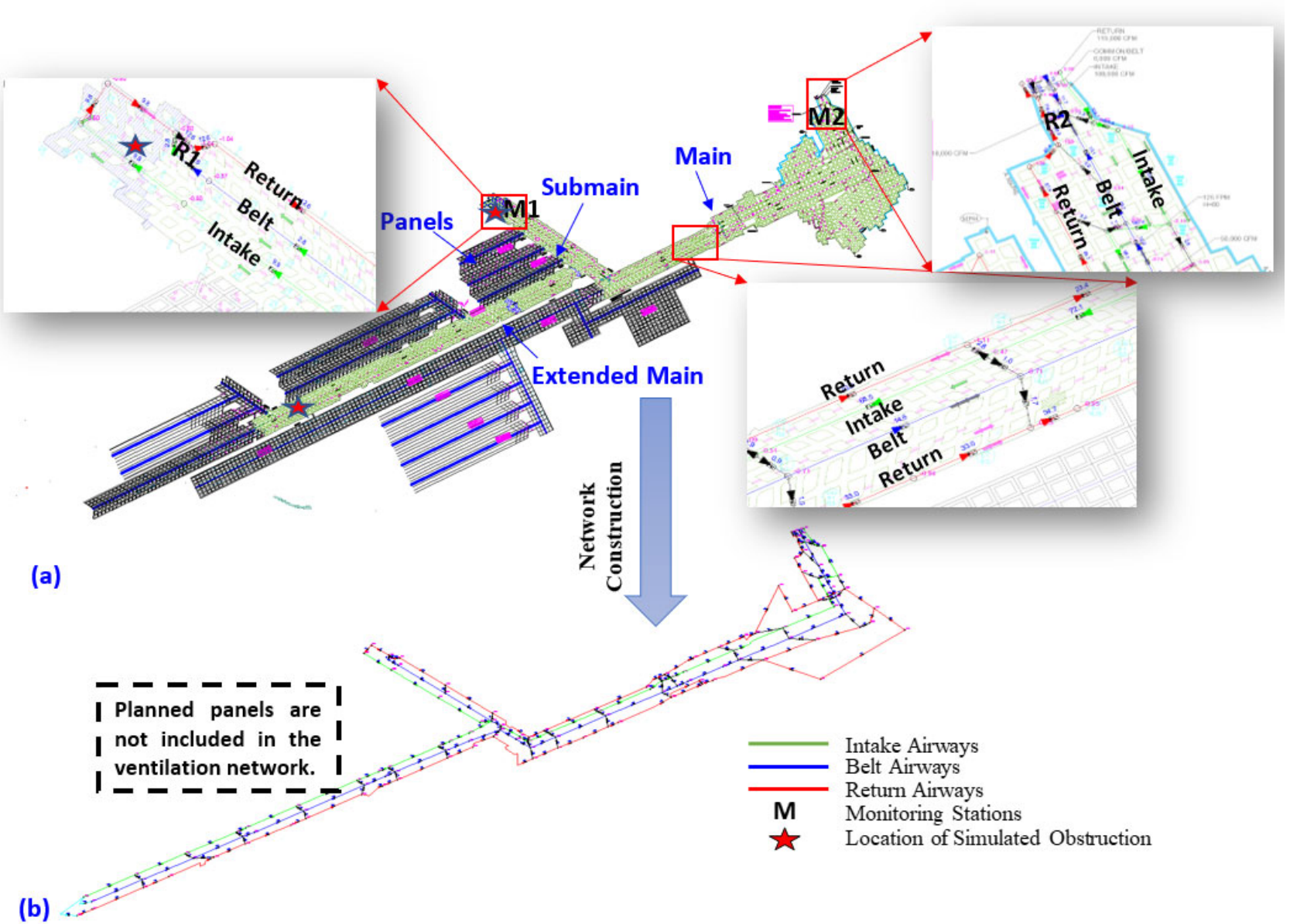

Figure 4-10. Small mine layout and corresponding ventilation network.

The results of ventilation network simulation with various roof fall incidents are listed in Table 4-2 and plotted Figure 4-11. The simulations demonstrated that different roof fall incidents can dramatically influence the airflow and air pressure distributions at this small mine. For the first scenario, the hypothetical roof fall occurs in the submain at the mouth of the panel, as illustrated in Figure 4-10. The differential pressure at monitoring point 1, M1, across Regulator 1 quickly dropped with respect to the resistance increase at the heading of the submain. This result can be explained by the resistance distribution of the overall mine. Since the overall resistance at the submain increased because of the roof fall at the heading, the total airflow delivered to the submain became restricted. According to the Square Law of ventilation frictional pressure drop, $\Delta p = R_{rg1}Q^2$, where Δp is the pressure drop across the regulator, R_{rg1} is the resistance of regulator, and Q is airflow through the regulator. The resistance across the regulator did not change, but the airflow through the regulator decreased because of the obstruction in the intake entry. Consequently, the differential pressure across the regulator decreased. For Regulator 2, the differential pressure slightly increased when the roof fall occurred in the submain region, as shown in Figure 4-11. The simulation results therefore support the conclusion that the roof fall incidents at the submain can be detected by pressure drops at both regulators. However, the effect was greater at Regulator 1, which was nearer to the incident than Regulator 2.

In Case 2, the roof falls occurred at the intake of the extended main, as shown in Figure 4-10. Calculations of pressure drops across the two regulators are illustrated in blue and pink dash lines in Figure 4-11. As the extent of the obstruction increases, the differential pressure measured at M1 (at Regulator 1) increases. This outcome is expected because the increased resistance in the extended main causes more air to split to the submain. For Regulator 2, a slight decrease of differential pressure was observed at M2, thus indicating an airflow decrease from the belt towards return. This case demonstrates that the differential pressure (airflow) measured at either regulator can capture subtle changes to the ventilation system even when they are installed relatively far from the incident location.

To compare the sensitivity of differential pressure for both regulators, the percentage change in differential pressure is plotted in Figure 4-12. The results indicate that the response of Regulator 1 (M1) is more sensitive than that of Regulator 2 (M2) for both roof fall incidents. As shown in Figure 4-12, the differential pressure across Regulator 1 (M1) increased by 61% in Case 2 and decreased by 95% in Case 1 when the resistance of roof fall branch is 1649R. By comparison, there was only a 12% increase in Case 1 and a 19% decrease in Case 2 for Regulator 2 (M2). These results suggest that ventilation variation is somewhat position-dependent and adjacent monitoring stations can effectively capture the ventilation changes in its regional area. Here, it should also be noted that the remote monitoring station, M2 for the small mine, can detect the change but it is challenging to determine the cause and specific location of the problem. Therefore, as explained earlier in this report, human intervention is required to determine the exact cause and location. Of course, a larger number of sensors could be distributed throughout the mine to aid in the exact location of the disturbance.

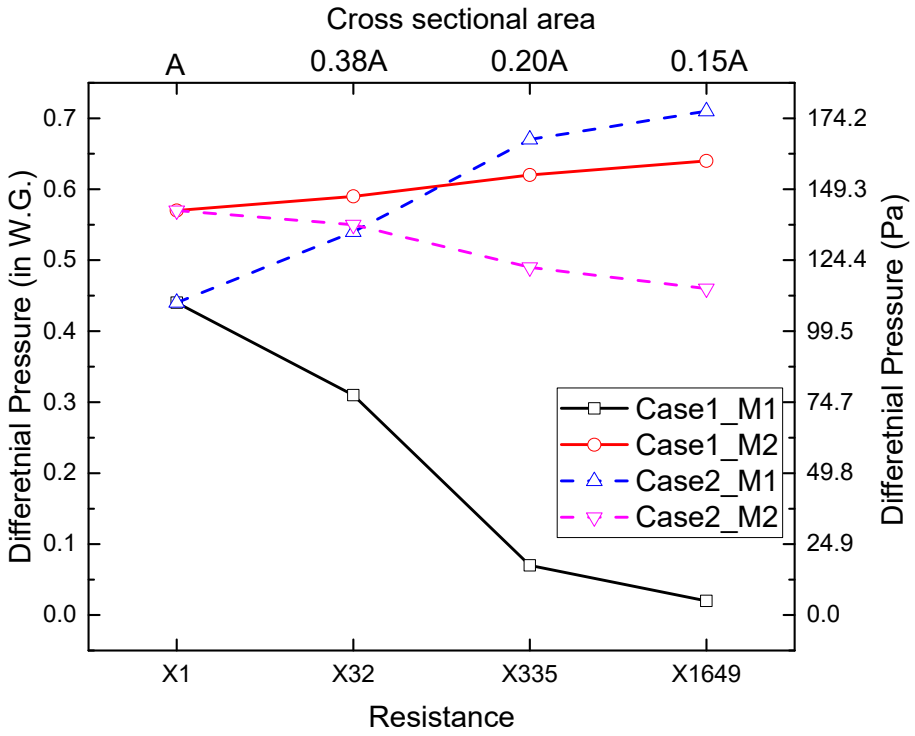

Figure 4-11. Plot of differential pressure at two monitoring regulators in roof fall incidents.

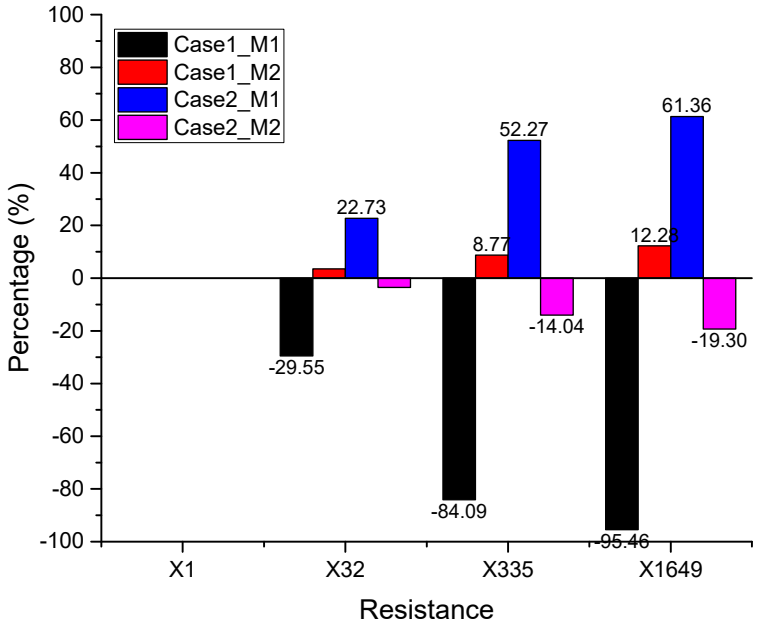

Figure 4-12. Percentage change of differential pressures at regulators for Cases 1 and 2.

The two scenarios described above indicate that the differential pressure data across the prescribed regulators can effectively capture the ventilation perturbations with different roof fall

incidents. Pressure sensors can be employed to identify the incidents in the mine to serve as sentinels for ventilation changes.

4.2.4.1 Simulation of excess leakage and unauthorized modifications of ventilation controls

In underground mines, necessary connections are made between intakes (belts) and returns at certain stages of mine development. When these connections are no longer required for access and/or ventilation, *stoppings* are built to prevent short-circuiting of the airflow. As the mine develops, abandoned areas of the mined-out regions are isolated from the active ventilation system and mine *seals* are constructed at the entrances of the connecting airways. At certain locations, where the access must remain available between an intake (belt) and a return airway, ventilation *doors* can be installed on the stoppings. A passive *regulator* is an adjustable orifice fitted onto a door or a stopping. Its purpose is to regulate the airflow to a desirable value in a given airway or section of the mine. The airflow can be adjusted by sliding the panel manually at the desirable position.

Among all of these doors and stoppings, there is ample opportunity for air leakage through the perimeter. If a mine has a moisture-sensitive roof and floor or weak ribs, the airways are liable to converge. This occurrence can potentially result in premature failure or cracking of the stoppings, which can lead to an excessive leakage between aircourses. Another cause of excessive leakage is opening a regulator to gain passage, and then forgetting to close it or return it to its original setting. Occasionally, miners on a section will change a regulator setting or prop open a door to gain additional air for their section. This change could have immediate consequences to other parts of the mine, and as such, it is crucial to understand how the sentinels can be optimized to respond to these changes or leakages. A series of ventilation simulations was conducted to check the differential pressure outcomes from various leakage conditions and regulator settings.

Two cases were simulated to represent potentially excessive leakage using ICAMPS-MineVent. The small mine was used as the example site. One case is an unauthorized man door opening, labeled C11 in Figure 4-13, and the other is a leak at the stopping between the intake and belt airways at the submain, labeled C12 in this figure. The leakage paths were added to the existing ventilation network for the simulation. In principle, different intensities of airflow leakage can be simulated by assigning different leakage path resistances. The lower the resistance of the leakage path, the higher the airflow leakage. In order to identify the resistance reduction for a progressively increased leakage, a conceptual model of equivalent leakage hydraulic diameter is introduced in Figure 4-14. The air leakage through a man door or a stopping is equivalent to the air going through a circular pipe with a diameter of d_0. The resistance drop due to leakage can be quantified as:

$$R_0 = C\frac{kL}{d_0^5} \tag{4-12}$$

where R_0 is the original airway resistance, which can be calculated based on the p-Q ventilation survey; d_0 is the initial equivalent airway hydraulic diameter; and C is the constant.

When the leakage path hydraulic diameter increases up to X times of d_0, (i.e., $d = Xd_0$), the resistance drops to $1/X^5$ of its original value:

$$R = C\frac{kL}{d^5} = \frac{1}{X^5}R_0 \tag{4-13}$$

By introducing this conceptual model of leakage resistance estimation, different cases of man door and stopping resistance drop were estimated and listed in Table 4-3. Seven of these cases (bolded in the table) were simulated using ICAMPS to check the responses of the pressure changes at the monitoring stations M1 and M2, which are shown in Figure 4-10 above.

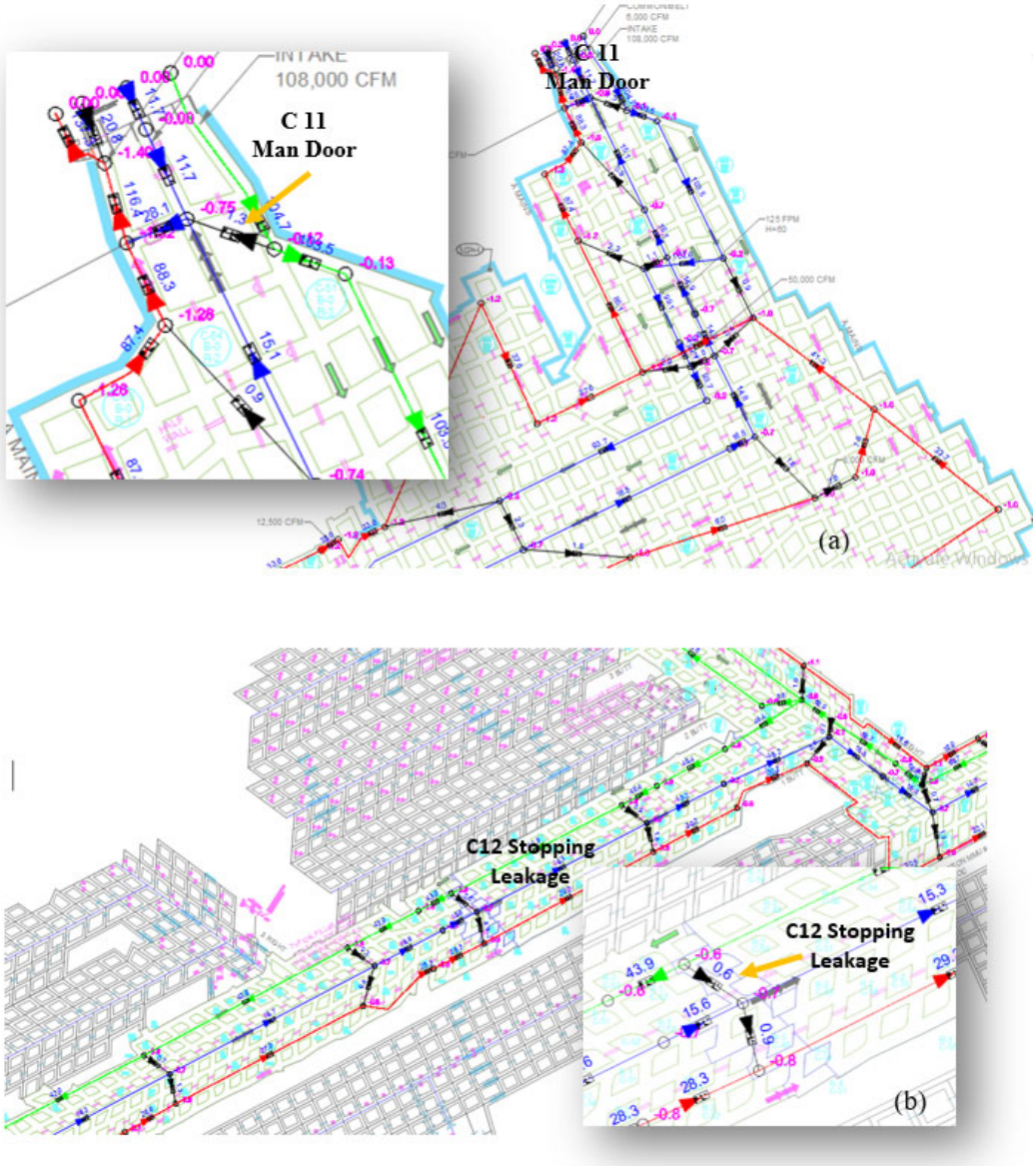

Figure 4-13. Man doors and stopping leakage positions on the mine map.

The resulting pressure drops are plotted in Figure 4-15. As shown for man door leakage in Figure 4-15(a), the pressure drops for M2 had an overall increase as the leakage increased, thus suggesting that the overall airflow delivered to the mine increased. This outcome was expected because the leakage airflow from the intake to the belt airway should provide additional airflow to the mine system. In other words, the belt airway behaved, to some extent, as a parallel intake entry, thereby decreasing the overall resistance for the intake airways. Given that the overall airflow increase contributes to the M2 pressure drop, these results show that M2 is an effective way to capture the airflow changes for the overall mine.

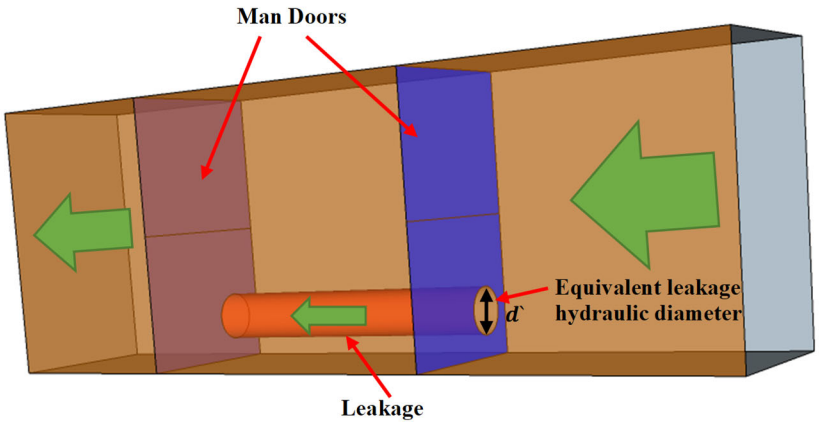

Figure 4-14. Illustration of airflow leakage through man doors in stoppings.

Table 4-3. Resistance values for rectangular airways with various width-height ratios.

No.	d/d0	Leakage area increase	Resistance reduction	C11 Resistance		C12 Resistance	
		A	R_0	original	new	original	new
1	1.05	1.1 A	78.35% R_0	4652.692	3645.506	1305.198	801.2781
2	1.1	1.2 A	62.09% R_0	4652.692	2888.956	1305.198	503.2102
3	1.2	1.4 A	40.19% R_0	4652.692	1869.813	1305.198	210.7967
4	1.3	1.7 A	26.93% R_0	4652.692	1253.105	1305.198	94.67662
5	1.4	2.0 A	18.59% R_0	4652.692	865.0956	1305.198	45.12278
6	1.5	2.25 A	13.17% R_0	4652.692	612.7002	1305.198	22.63412
7	1.6	2.56A	9.54% R_0	4652.692	443.7153	1305.198	11.8707
8	1.7	2.89 A	7.04% R_0	4652.692	327.6874	1305.198	6.474214
9	1.8	3.2 A	5.29% R_0	4652.692	246.2305	1305.198	3.655537
10	1.9	3.61 A	4.04% R_0	4652.692	187.9041	1305.198	2.128826
11	2	4 A	3.13% R_0	4652.692	145.3966	1305.198	1.274607
12	3	9 A	0.41% R_0	4652.692	19.14688	1305.198	0.022104
13	4	16 A	0.10% R_0	4652.692	4.543645	1305.198	0.001245
14	5	25 A	0.03% R_0	4652.692	1.488861	1305.198	0.000134
15	6	36 A	0.01% R_0	4652.692	0.59834	1305.198	2.16E-05
16	7	49 A	0.01% R_0	4652.692	0.276831	1305.198	4.62E-06
17	8	64 A	0.00% R_0	4652.692	0.141989	1305.198	1.22E-06

Notes: d – equivalent leakage hydraulic diameter; A – cross section area of leakage circle; R_0 – original resistance of doors (stoppings).

However, the results for M1 fluctuate in different conditions. This outcome was also expected because the M1 is located at the end of the submain, where it can only capture the local changes. Moreover, the quantity of the airflow delivered to the submain was partially determined by the free split between the submain and the extended main. In effect, the airflow to the submain is not only determined by the submain but also by the variation of the extended main.

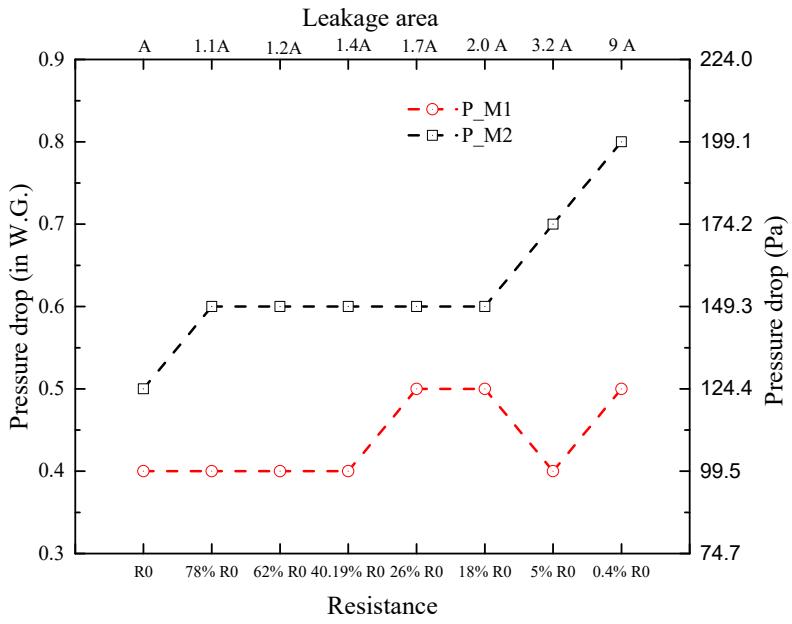

(a) Case study results of main door air flow leakage (A - initial equivalent area and R_0 - initial resistance of leakage entry)

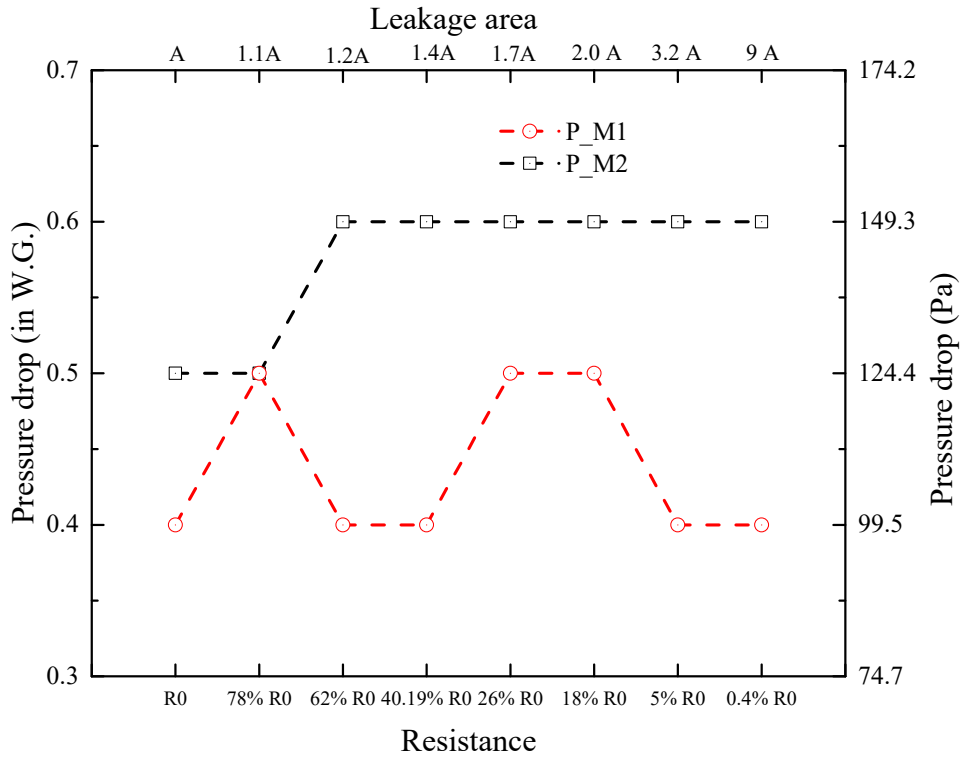

(b) Stopping air flow leakage at extended main (A - initial equivalent area and R_0 - initial resistance of leakage entry)

Figure 4-15. Results of pressure drop and airflow at monitored spots in different resistance reduction cases.

For the stopping leakage, the pressure drops at M1 and M2 are plotted in Figure 4-15(b). As with Case 11, the pressure drop for M2 near the portal increases when excessive airflow leakage occurs at the extended main. The M1 station at the end of the submain changes with airflow leakage at the extended main. The increased pressure drop at M2 occurs because the leakage makes the belt entry behave as a parallel airway to the intake, resulting in a decrease in the overall resistance of the extended main. However, comparison of both cases reveals that there was a total of 0.3 in water gauge (W.G.) pressure drop (0.8-0.5) for Case 11 and 0.1 in W.G. increase for Case 12. This difference resulted from the overall mine resistance change. In Case 11, a much longer belt airway behaved as a parallel intake entry because it started from the portal to the end, whereas in Case 12, it only influenced the branches at the extended main. Consequently, Case 11 should have a higher pressure drop than Case 12. In both cases, the M1 station was not effective in capturing the airflow leakage because it did not yield consistent results. Therefore, the simulation results indicate that low levels of air leakage cannot be detected.

In addition to studying the pressure changes at the two monitoring stations, M1 and M2, the influence of the leakage on fan performance was examined in order to determine whether fan pressure can be used as a sentinel for airflow leakage. The results are shown in Figure 4-16. Evidently, the man door leakage had a much stronger impact on the fan pressure compared to the stopping leakage at the extended main. The increasing leakage led to a drop of fan pressure and an increase of airflow because of the overall decrease in mine resistance. A change in the fan pressure was not observed for stopping leakage because this leakage only influences pressure locally. In sum, fan pressure can be used only to detect a significant short circuit or leakage, in which the leakage results in a decrease to the overall mine resistance; otherwise, this sentinel (at the fan) is not sensitive enough to capture airflow leakage.

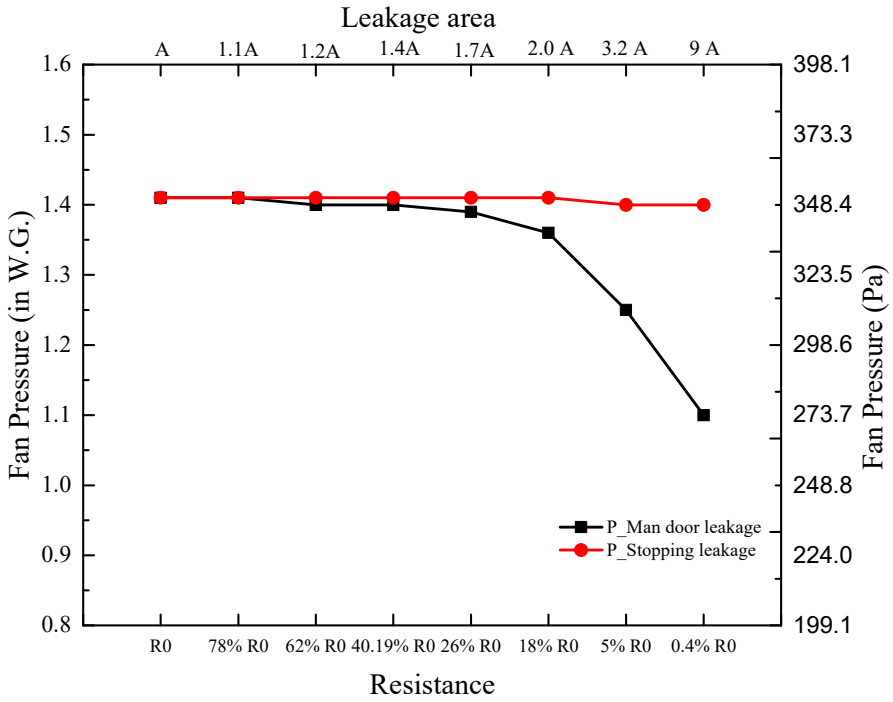

Figure 4-16. Results of fan performance at monitored spots in different resistance reduction cases.

4.2.5 Large Mine Simulation Studies

The important difference between a "small" and "large" mine, for the purposes of this project, is that the large mine has one longwall or more. The monitoring strategies examined in the previous sections of this report apply to any size of mine. The location principles articulated apply to the continuous miner sections used for mains and panel development in a large mine. Of course, it was necessary to build the mine ventilation model for the large mine used for these studies. This was the same as described above: the AutoCAD-specified network was input into MineVent, and then the *p*-*Q* survey data for that mine was used to adjust the model parameters. Once sufficient agreement was obtained between the model predictions and the observed ventilation survey results, these model results were used as the base case for the subsequent simulations. This mine had seven sealed longwall panels, one working panel, one developed panel, and a bleeder system, as shown in Figure 4-17.

The ventilation network for a large-scale longwall operation with multiple panels can be very complicated. Each longwall district will have a bleeder fan and often there are multiple portals. This complexity can be seen in Figure 4-17. Nonetheless, the key events of interest on a longwall operation are ensuring that the design-level of intake air is available to the longwall face and ensuring that air movement at the t-split is according to the design (approved plan) values. Sentinels to detect problems that are affecting these airflows were described in Section 4.1 and shown in Figure 4-6.

For the purposes of this large mine simulation, two monitoring stations were selected as shown in Figure 4-17. One (M1) is at the regulator between fresh and return aircourses in the tailgate at the T-split and the other (M2) is located at the regulator in bleeder system at the active panel. The locations of these two cases are shown in Figure 4-17.

Two locations were selected to introduce disturbances to the system, i.e., obstruction of the aircourse: one a midface of the longwall and another in the center (#2) entry of the tailgate bleeder. The locations of these two cases are illustrated in Figure 4-17.

Induced resistance changes were simulated in the same fashion as for the small mine case and the pressure changes across the regulators were examined. The sensitivity of the sentinels was then analyzed. The resulting differential pressures at each monitored location, for each of the cases and resistance values, are summarized in Table 4-4. The resulting differential pressures at M1 and M2, for each case and differing levels of obstructions, are plotted in Figure 4-18. The percentage changes in pressure at each of the monitored locations, for each case and each level of resistance, are shown in Figure 4-19.

Table 4-4. Results of differential pressures at M1 and M2 for different resistances for each case.

Roof fall pilots	Cross sectional area	Resistance	Differential pressure at M1	Differential pressure at M2
	A	R_e	1.74	3.42
Case1	0.38A	32.00 R_e	0.87	3.4
(Working	0.21A	335.54 R_e	0.33	3.38
panel)	0.15A	1649.16 R_e	0.26	3.38
Case 2	0.38A	32.00 R_e	1.5	3.06
(Center entry	0.21A	335.54 R_e	1.43	2.95
of bleeder system)	0.15A	1649.16 R_e	1.42	2.91

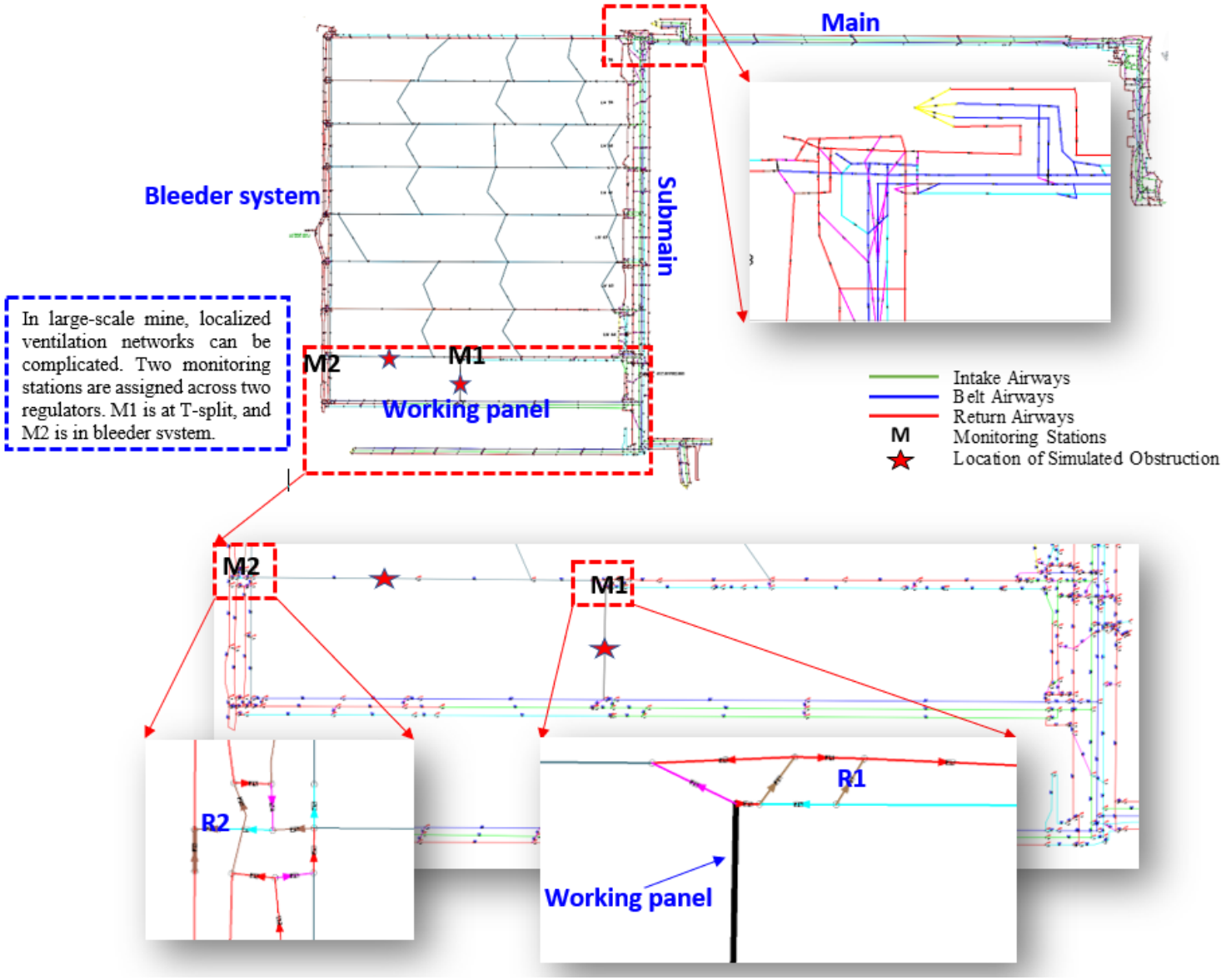

Figure 4-177. Large mine layout ventilation network with monitoring stations.

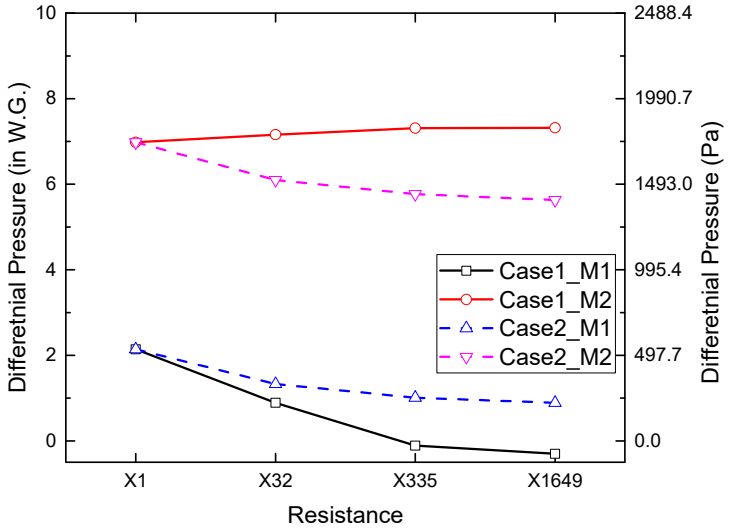

Figure 4-18. Differential pressure at regulators for each case and for different levels of resistance.

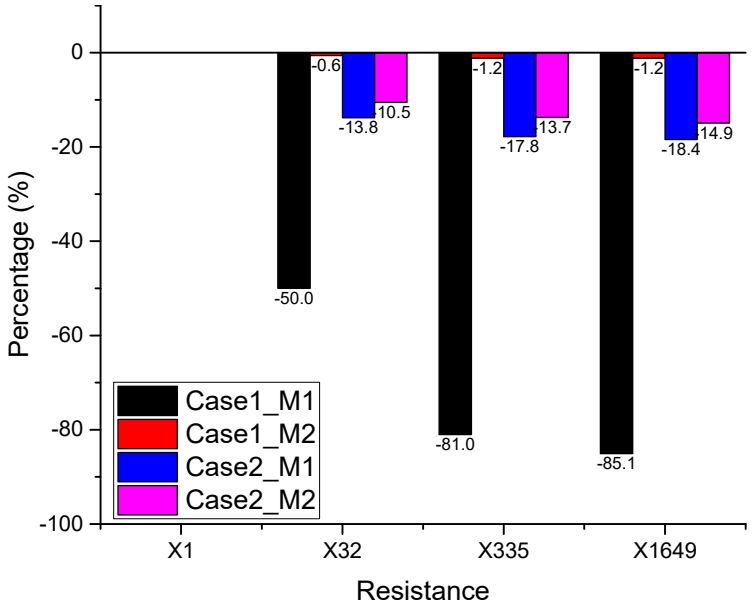

Figure 4-19. Percentage change of differential pressures at the monitored locations for each case study.

In Case 1 with an obstruction at midface of the longwall, differential pressure across R1 slightly decreased as the obstruction increases. Reduced airflow at working panel leaded to differential pressure drops for both M1 and M2 for regulator R1 and R2 as shown in Figure 4-18. The differential pressure across R2 showed an obvious decrease. In Case 2 with obstruction the center (#2) entry of the tailgate bleeder, the total amount of air went through #2 entry of the tailgate decreased. Because of the limited airflow toward the bleeder entry, more airflow was forced to pass through the return at the tailgate and therefor, pressure at return aircourse in the tailgate increases and correspondingly the differential pressure across R1 is found to be decreased as illustrated in Figure 4-18. For both cases, the differential pressures at both T-split and bleeder system were found to be decreased with both types of airway obstructions. These simulation results suggest the differential pressure monitoring at the two designate regulators can serve as effective sentinels to alert mine personnel to the need for closer examination when pressure drops.

Similar to observed results for the small mine, the monitoring position closest to the introduced disturbance is more sensitive to changes than more distantly located sentinels. In Case1, the differential pressure at M1 was 85.1% smaller than its initial value when the longwall face increase for 1649R. However, the influence at M2 was negligible. In Case 2, both monitoring stations at the regulators can effectively capture the converge of center entry at the bleeder. The highest reduction of pressure drop at M1 was 18.4% with the 1649R, and the largest reduction of that at M2 was 14.9%, as shown in Figure 4-19.

4.2.6 Differential pressure drop at the designated regulator for small and large mines

To quantitatively estimate the variations of pressure drops under various ventilation interruptions, the small and large mine examples were discussed here. The validated mine ventilation models discussed in Section 4.2.1 were used to obtain the *in situ* regulator resistances and initial airflows.

For the small mine, C11 regulator was selected for the analysis and the resistance and airflow were listed in Table 4-5 and the location of the regulator is shown in Figure 4-13. The initial pressure drop is 109.5 Pa. If the airflow reduced by 70% (12.6 kcfm × 70% = 8.82 kcfm ≈ 9,000 cfm), the pressure drop becomes 10.7 Pa. For regulator C11, it indicates that the pressure change is 98.8 Pa (109.5 – 10.7 = 98.8 Pa) with approximate 9,000 cfm airflow change through this regulator. This can be easily captured by the developed instrument with accuracy of 2 Pa as detailed in Appendix II.

For the large mine, M1 regulator was selected for the analysis and the resistance and airflow were listed in Table 4-6 and the location of the regulator is shown in Figure 4-17. The initial pressure drop is 532.5 Pa. If the airflow reduced by 30% (32.6 kcfm × 30% = 9.78 kcfm ≈ 10,000 cfm), the pressure drop becomes 259.2 Pa. For regulator M1, it indicates that the pressure change is 273.3 Pa (532.5 – 259.2 = 98.8 Pa) with approximate 10,000 cfm airflow change through this regulator. This also can be easily captured by the developed instrument with accuracy of 2 Pa as detailed in Appendix II.

Table 4-5. Small mine regulator pressure drop data for C11 regulator

Airflow drop	ΔP (Pa)	ΔP (in w.g.)	Q (kcfm)	R (in min^2/ft^6)
0	109.5	0.4	12.6	30.0
10%	96.0	0.4	11.3	30.0
30%	58.1	0.2	8.8	30.0
50%	29.6	0.1	6.3	30.0
70%	10.7	0.0	3.8	30.0
90%	1.2	0.0	1.3	30.0

Table 4-6. Large mine regulator pressure drop for M1 regulator

Airflow reduction	ΔP (Pa)	ΔP (in w.g.)	Q (kcfm)	R (in min^2/ft^6)
0	532.5	2.1	32.6	20.0
10%	428.4	1.7	29.3	20.0
30%	259.2	1.0	22.8	20.0
50%	132.2	0.5	16.3	20.0
70%	47.6	0.2	9.8	20.0
90%	5.3	0.0	3.3	20.0

4.3 In-Mine Validation Experiments

The results of the simulations, which used validated ventilation models, demonstrate the utility of the proposed sensor location strategy. At the same time, these results confirm the hypothesis that pressure monitoring is superior to air velocity monitoring as a surrogate measure for air quantity. Nonetheless, an in-mine validation would further strengthen the confidence in the project recommendations.

Designing in-mine experiments to test the validity of the recommendation is simple in theory. Sensors would be located at the proposed locations for sentinels, event scenarios would be simulated, and the collected data analyzed. Simulation of event scenarios could be accomplished by creating artificial obstructions, e.g., using foam boards to block 10% of the airway's cross-sectional area, partially opening a mine door, or making a small adjustment to a regulator. In practice, such experiments are fraught with problems. The primary difficulty is that any change in airflow greater than 9000 cfm from the plan values requires withdrawing the miners and notifying MSHA. In this light, it is not surprising that mining companies were unwilling to allow these experiments to be conducted in their mine. Alternatives were considered, including conducting the experiments when there were no production or maintenance activities in the mine, but these alternatives were deemed unworkable for various reasons.

The Pittsburgh Mining Research Division (PMRD) of the National Institute for Occupational Safety and Health (NIOSH) and its predecessor, the U.S. Bureau of Mines, encountered practical barriers to the in-mine experimentation that was critical to their research programs. They developed two world-class experimental mines to facilitate research: the Safety Research Coal Mine (SRCM) and the Lake Lynn Laboratory (LLL). Discussions were initiated with NIOSH PMRD staff, and after review and discussion, including with MSHA, approval was given to conduct experiments in the SRCM located at their main campus in Bruceton, PA.

The goals of the in-mine study at the SRCM were to simulate the event scenarios, to assess the efficacy of the sensor location strategy, and to evaluate the effectiveness of using pressure monitoring to detect incipient problems in the mine ventilation system during routine operations. These goals were achieved through the field-scale experiments, computational fluid dynamics (CFD) modeling, and analyses of the results from both activities.

4.3.1 Background of CFD modeling

McElroy and Kingery (1957) first provided guidelines on the value of ventilation pressure surveys and the instruments and method for conducting the surveys. Their early work discussed the practical application of pressure data and factors that could influence the survey data. Later, Wala et al. (2005; 2007) conducted comprehensive lab studies on the velocity profiles around a continuous miner operating in a room and pillar panel. They tested three different turbulence models and found good agreement with the experimental data. This early work in CFD demonstrated that CFD was a viable alternative to expensive and often difficult field-scale experiments.

CFD ventilation modeling was used by Sasmito et al. (2013) to simulate gas concentrations and pressure loss from four different stopping arrangements in room and pillar workings. The CFD modeling was validated from experimental work, although the data were not presented in the publication. Xu et al. (2013) created a novel longwall-mine model and were able to locate an obstruction using tracer gas through lab testing and numerical CFD simulations. Xu and colleagues

(Xu, Jong, Luxbacher, & Mcnair, 2015; Xu et al., 2015) used CFD models to determine tracer-gas release rate, duration, and the best release locations. In conjunction with the concentration plots, these studies provided guidance for the use of CFD models in the design of field experiments. Subsequently, the researchers used in-mine tracer-gas studies in conjunction with CFD to evaluate the state of four different localized ventilation scenarios and found that CFD-predicted results agreed with measured concentrations. However, detailed ventilation surveys are needed to calibrate these models before any predictions can be made.

The foregoing studies demonstrated that CFD is a powerful tool for determining ventilation system performance and corroborating in-mine findings.

4.3.2 Experimental Plan at the SRCM

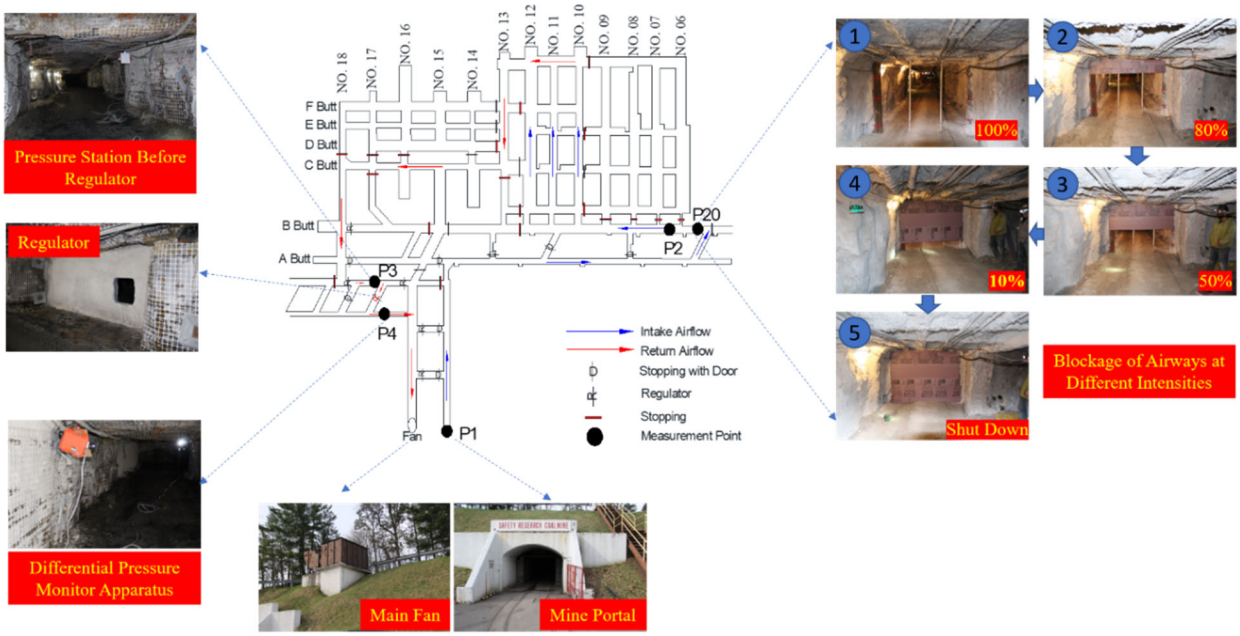

Figure 4-20. Safety research coal mine layout and ventilation monitoring stations.

The layout for the part of the SRCM used for the experiments is shown in Figure 4-20. Locations for five monitoring stations were identified, as labeled in Figure 4-20. Six different event scenarios were devised, each representing a problem that could develop in a mine ventilation system. At the appropriate time, each scenario was implemented in the mine, and pressure and air velocity measurements were recorded at the five monitoring stations.

Five of the scenarios consisted of varying degrees of airway obstruction and one consisted of a leakage (short circuit). The short circuit was created by opening a door between the intake and return entries at the second crosscut from the portal, as illustrated in Figure 4-21.

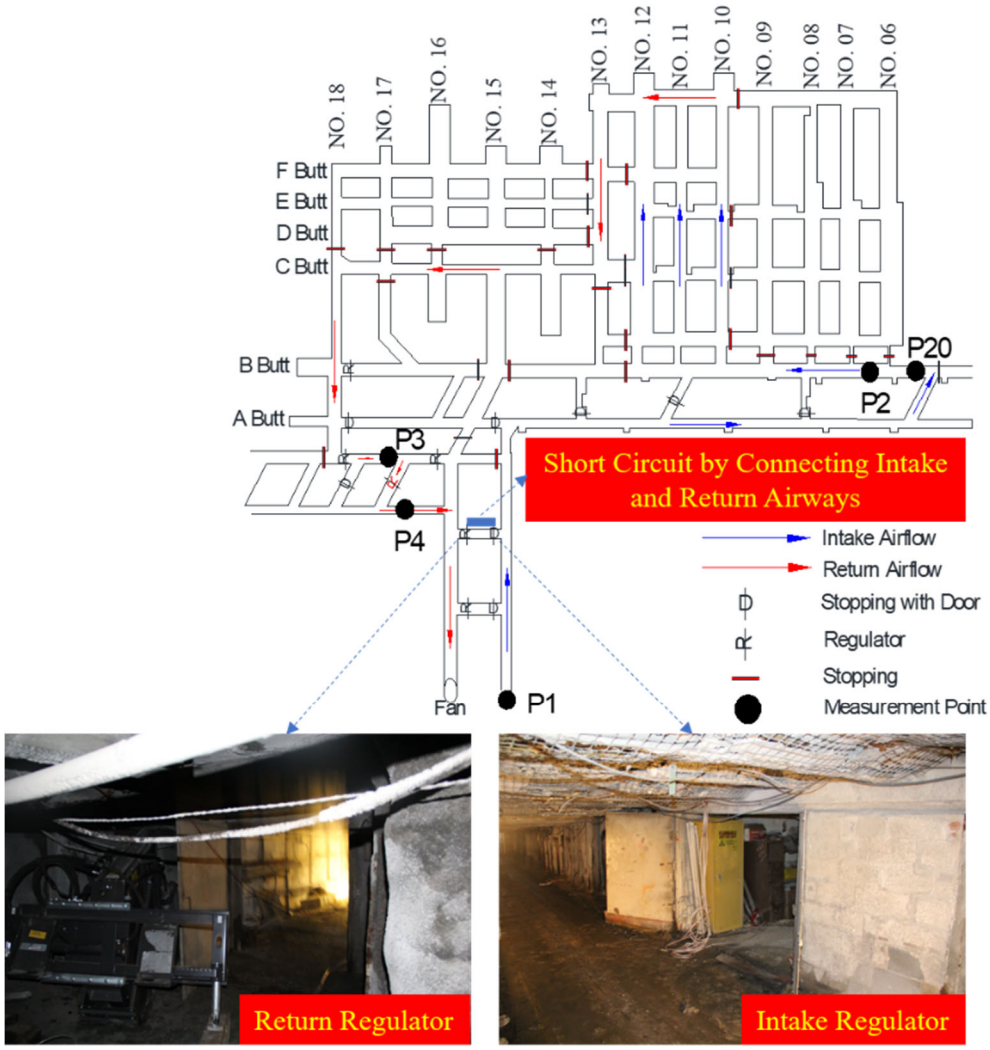

Figure 4-21. Location of the mine doors that were opened to create the short-circuit path.

The effect of an airway obstruction was created by using foam boards to block a part of the entry. A frame was constructed around the perimeter of the entry between the P2 and P20 monitoring stations. Specifically, this "resistance fixture" was located in the B-Butt entry between the No. 6 and No. 7 crosscuts, as shown in Figure 4-20. No resistance (foam board) was placed for the first experiment. In the second through fifth experiments, foam boards were inserted to obstruct 20%, 50%, 90%, and 100% of the airway. All foam boards were removed for the sixth experiment and the short circuit was created by opening the mine door between the main intake and return, as shown in Figure 4-21.

Absolute barometric pressure was measured at stations P1, P20, P2, P3 and P4 using altimeters. All the altimeters were calibrated in the laboratory before the in-mine experiments. The differential pressure was monitored and recorded using our developed data acquisition and pressure monitoring system.[9] Differential pressure was measured in the following locations: between P3 and P4, which is across regulator R1; between P4 and P6, which is across regulator R2; and between P3

[9] The specifications of data acquisition and pressure monitoring system were described in detailed in the Appendix I – A 1.1.

and P6, which provides a check on the measurements across R1 and R2, because this pressure should be equal to the sum of the measured differential pressures across R1 and R2. These locations are shown in Figure 4-22. Differential pressures were measured using pressure transducers and the values were continuously recorded on the data logger described in Section 4.1.2. The data logger was located at station P4 and rubber tubing was used to connect the pressure transducers to the requisite points in the mine. The air velocity at stations P1, P2, P3, and P4 was measured using a vane anemometer (continuous traverse).

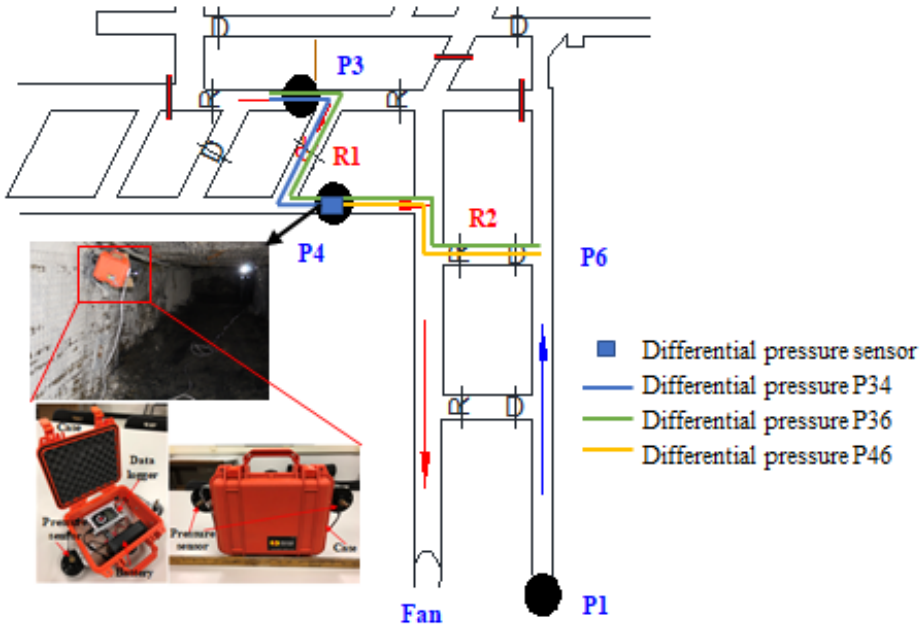

Figure 4-22. Differential pressure measurements between different monitoring stations.

4.3.3 CFD Model Establishment

A field-scale CFD model was established based on the mine map for the SRCM. The model dimensions are shown in Figure 4-23. One inlet was set as the intake entry and one outlet was set as the return entry. To mimic the real mine situation, the CFD model was built as an exhausting ventilation system. Differential pressure was used as the initial condition for the CFD model. The average differential pressure between the exhaust entry and the intake portal was ~380 Pa according to the field ventilation survey. Therefore, the initial total pressure at inlet was 380 Pa and 0 Pa at outlet. To simulate the wall roughness-induced pressure drop along the air-flow direction, the equivalent roughness in the model was set as 0.0001 m through trial-and-error experiments. Temperature effect was not considered in this model because the temperature and humidity were assumed constant during the period of field investigation. Turbulent flow was applied using the $k-\varepsilon$ turbulence model. Stoppings and regulators were simulated by blocking the airways and/or reducing the cross-sectional area, as shown in Figure 4-23. Different scenarios were simulated by adjusting the opening area of the artificial obstruction. For each ventilation interruption, both pressure and air velocity profiles were reduced from the equilibrium CFD model results, and the model results were compared against the in-mine observations. This process is described in the next section.

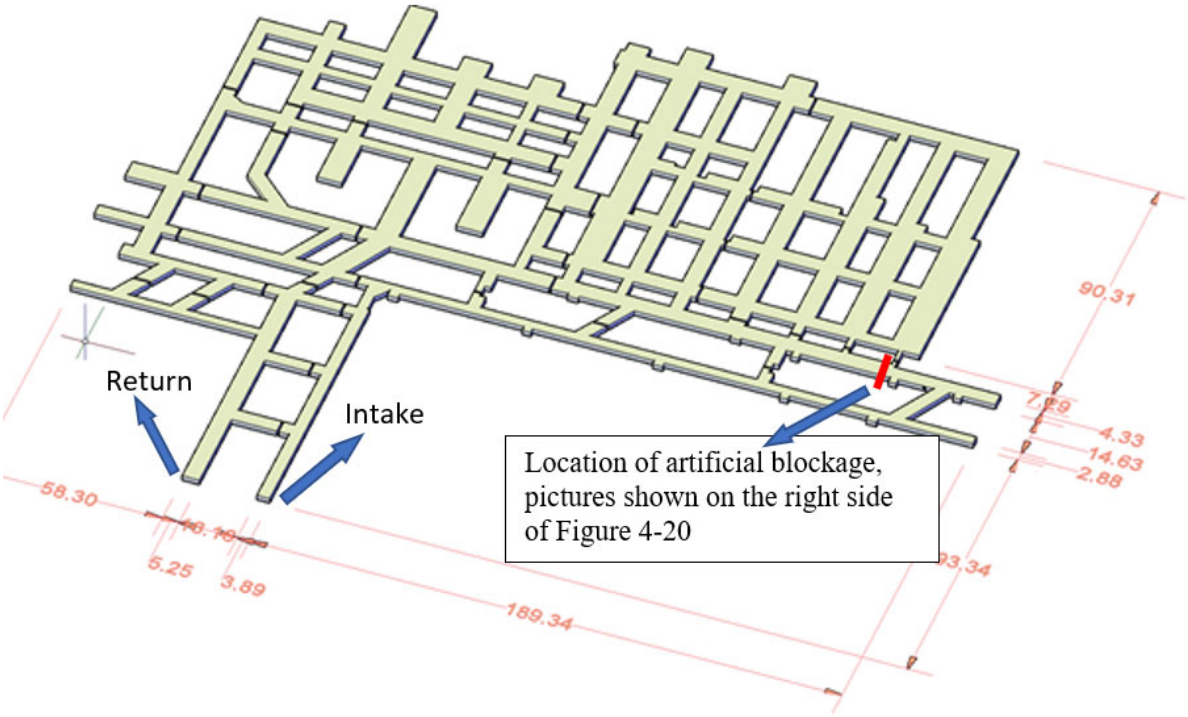

Figure 4-23. 3D CFD model of the Safety Research Coal Mine (unit-meter).

4.3.4 Results and Discussion of the In-Mine Experiments and Simulations

4.3.4.1 Pressure and velocity

The barometric pressure readings at all five monitoring locations are plotted in Figure 4-24. These pressures were calculated directly from the measured altitude readings. Figure 4-24 shows that the atmospheric barometric pressure (P1) decreased from morning to noon because of the temperature increase during that interim. This result confirms that the altimeter barometric pressure survey can accurately monitor the background atmospheric barometric pressure change. For each obstruction condition, from 100% open to fully closed, the pressure consistently decreased from the intake portal to the return P4, as illustrated by the shaded arrows in Figure 4-24. These results validated the ventilation Square Law that the pressure continually decreases because of the frictional pressure drop along the airways. In the case of airflow short circulation, the pressure at P20 was close to the pressure at P2 for two reasons: (1) because of the airflow circulation, very limited airflow went into the mine and instead passed directly from P6 to the return; and (2) because the airway is fully open, negligible resistance occurred between P2 and P20. Therefore, the pressures were expected to be the same as shown in Figure 4-24. However, the absolute pressure values at P20 and P2 are smaller than that of the 100% open case. The measured results indicate that the altimeter readings were quite stable and accurate in capturing the insignificant pressure variations in underground mines.

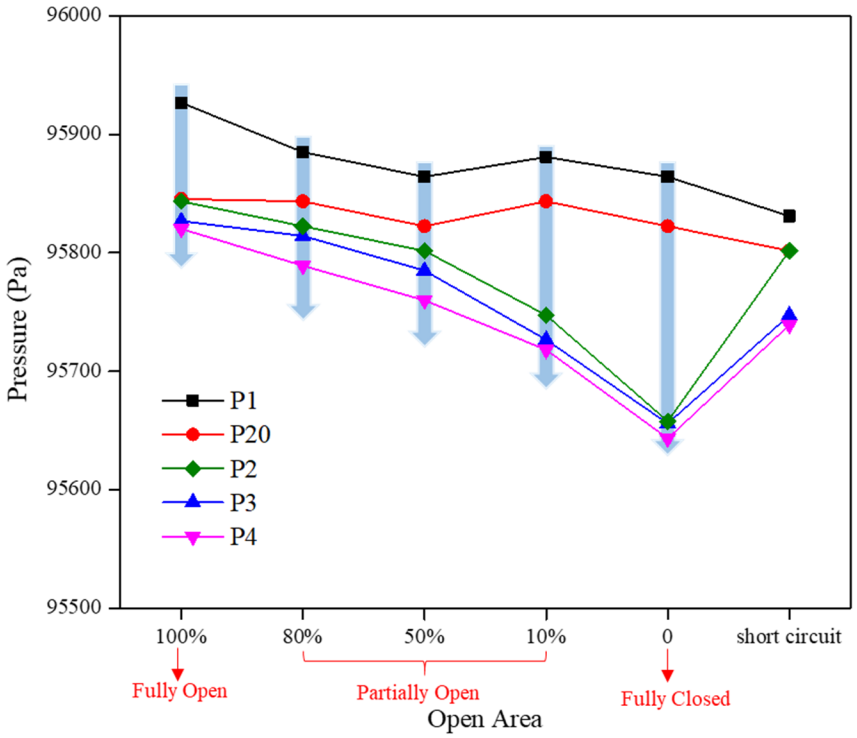

Figure 4-24. Pressure at monitoring positions with various ventilation interruptions.

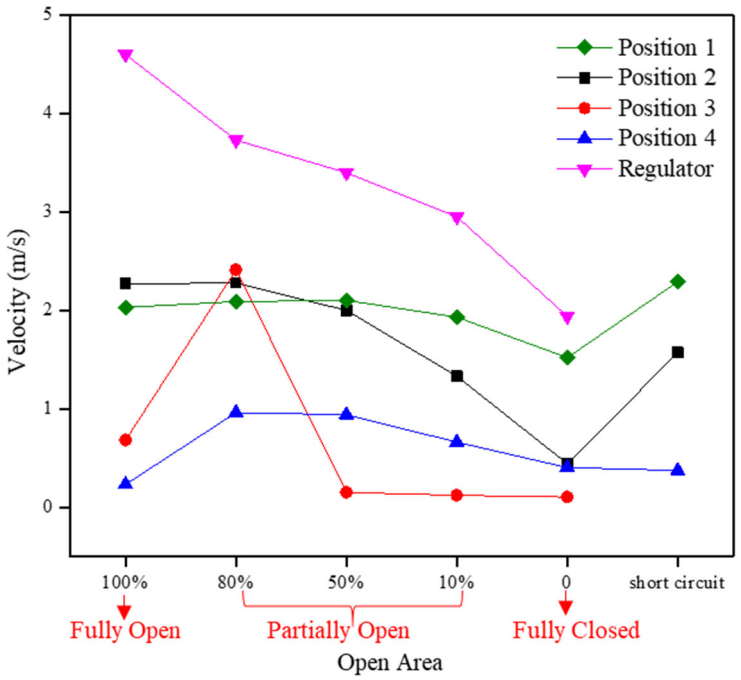

Figure 4-25. Velocity at monitoring positions with various ventilation interruptions.

Figure 4-25 shows the velocity measurements taken at each of the 4 positions and at the regulator. It is not surprising that the most reliable velocity data were taken at the regulator, which shows a monotonic decreasing trend (pink line) with continuous blockage for the intake airway. However, the measured velocities at different locations show a fairly scattered pattern. The velocity at

position 2 (black line) remains relatively constant until 100% of the open area is blocked, then an immediate decrease occurs. Furthermore, the air movement at position 3 is very limited because position 3 is a very large opening compared to other entries. Therefore, negligible air velocity can be accurately measured after a 50% blockage. In comparison, the regulator still records airflow. Positions 1 and 4 show a relatively constant velocity with the exception of the 100% blockage condition. It can be inferred from these results that velocity monitoring enables sizable errors because the velocity is subject to local influences. However, the pressure is stable and easy to interpret for the ventilation changes.

4.3.4.2 Differential pressure

The results in continuous differential pressure from varying ventilation interruptions are plotted in Figure 4-26. At each ventilation interruption scenario, all three differential pressures (P_{46}, P_{34}, and P_{36}) were monitored over a period of time. Small variations were observed for all differential pressures after they reached equilibrium. The few sharp peaks that occurred were believed to be caused by the sudden change of pressure from temporarily opened doors or mine personnel passing nearby on foot or in vehicles. The stable and equilibrium pressure data were used for the subsequent analyses. The trends for both P_{46} and P_{36} increased with the reduction of the opening size, although P_{36} data in some cases show fluctuations before it reached its steady state. By contrast, a continuous decreasing trend was observed for P_{34}, where the obstruction is out of this pressure region and cannot directly influence the resistance between P3 and P4. The results in Figure 4-26 closely related to the trends shown in Figure 4-24. These results demonstrate that the pressure monitoring is more reliable and consistent than the velocity measurements.

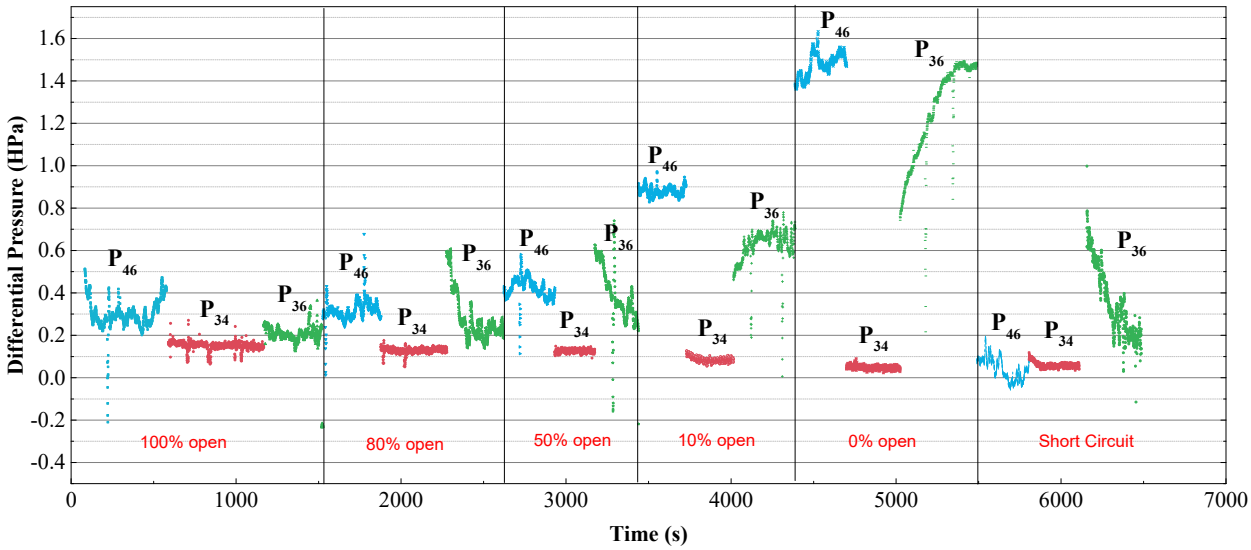

Figure 4-26. Differential pressure data across regulators with various ventilation interruptions.

Figure 4-27 shows the average data from the differential pressure monitoring locations P_{46}, P_{34}, and P_{36}. It is apparent that P_{46} and P_{36} systematically increased with progressive blockage of the airway since the resistance increases accordingly. Once the obstruction reached 100% blockage, P_{36} and P_{46} increased to approximately five and six times their original values. Interestingly, P_{34} decreased as the blockage increased. This value was expected to decrease because the airflow going through the airway from P3 to P4 drops and the resistance between P3 and P4 remains the same, thus reducing the differential pressure between two stations.

From Figure 4-27, it can also be concluded that differential pressure can be used to capture short circulation, as P_{46} tended to be zero because of open doors between return and intake. Similarly, P_{36} decreased to a minimal value because less air went through the mine. These results show that the differential pressure can be used to infer the location of the incident with certain confidence. For example, in the airway blockage scenario, the lack of change in P_{34} means that the blockage was not located between P3 and P4. This will inform the operator that the ventilation interrupt occurred between P3 and P6. In the case of short circulation, the P_{46} was almost zero, thereby signaling that the short circulation occurred between P4 and P6.

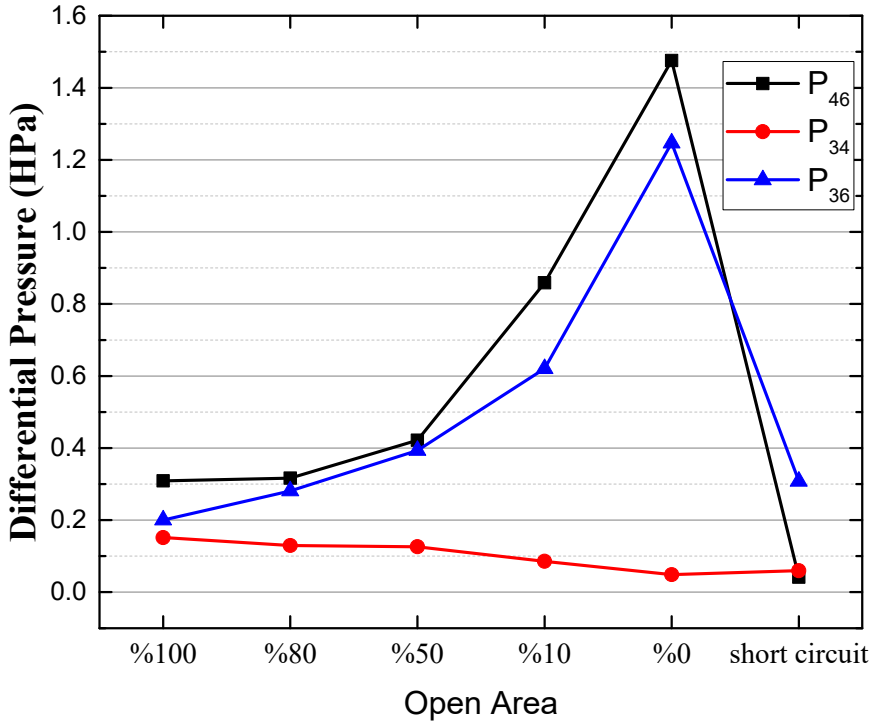

Figure 4-27. Differential pressure with various ventilation interruptions.

Figures 4-28 and 4-29 show the differential pressures in several locations between monitoring stations, P_{202} (=P20-P2), the regulator P_{34} (=P3-P4), and P_{14} (=P1-P4). Pressure monitoring data across the entire section (P_{14}) show the increasing pressure trend as air blockage increased. Therefore, pressure can be used as a sentinel and precursor of ventilation interruption for the whole mine. As soon as ventilation interruptions were noted, the next step was to determine the causes and locations.

The differential pressure across the regulator was defined by P_{34} and did not involve any ventilation interruption between P3 and P4. P_{202} was used to define the pressure drop between P20 and P2 because of the artificial airway blockage. As described above, P_{202} had an obvious increase but P_{34} slightly decreased. In order to identify where the ventilation interruption occurred, the increased percentages of differential pressures were plotted in Figure 4-29. Evidently, if the interruption position is between the two positions where the differential pressure is monitored, the differential pressure increase induced by the resistance increase is reflected by an increasing area, as can be seen for P_{14}. Similarly, if the interruption position is not located between the two monitoring locations, the differential pressure decreases slightly because of the corresponding airflow reduction, as observed for P_{34}. P_{202} shows a significant increase because the air blockage occurred

between P2 and P20. By monitoring and analyzing the differential pressure results, operators can easily narrow down the potential ventilation interruptions and identify the probable location.

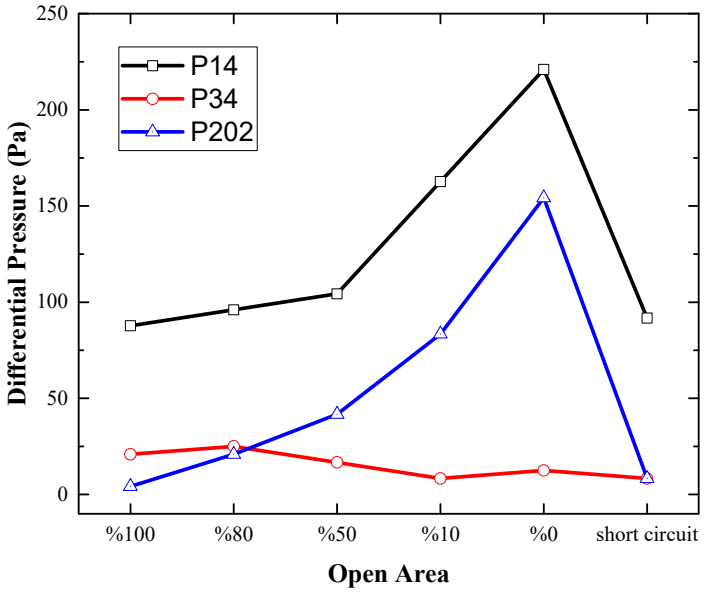

Figure 4-28. Differential pressure between monitoring positions with various interruptions.

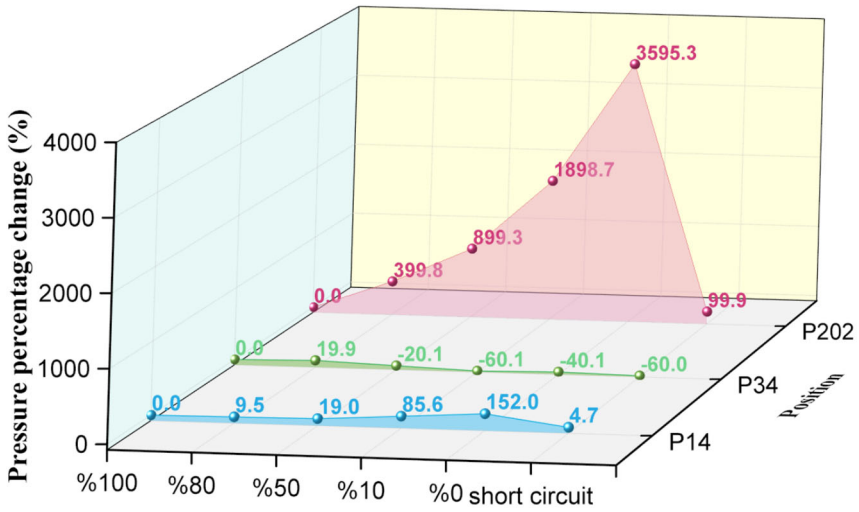

Figure 4-29. Pressure percentage change of differential pressure with reducing open area.

4.3.4.3 Theoretical analysis of differential pressure

The Square Law is the single most important equation in subsurface mine ventilation to estimate the airway resistance from frictional pressure drop (p) and airflow (Q) data obtained from the ventilation survey. The relationship between pressure drop and resistance can be expressed as:

$$p = RQ^2 \text{ or } P_{ij} = \Delta p = RQ^2 \quad (4\text{-}14)$$

where P_{ij} is the differential pressure from position *i* to position *j* (McPherson, 1993). The parameter *R* is the resistance of the airway system based on Atkinson's equation. From the equation, the frictional pressure drop is determined by both the resistance and airflow.

Resistance *R* is the function of airway geometry and roughness if it is assumed that the passing air is incompressible. Given an airway with certain geometry, the resistance can be written as:

$$R = kL\frac{per}{A^3} \tag{4-15}$$

where k is friction factor, *L* is the length, *per* is the perimeter, and *A* is the cross-sectional area.

Based on the two equations above, the geometry-change-induced ventilation interruptions can either increase or decrease the localized resistance, and the airflow will thus be passively and slightly adjusted if surface and fan pressure are assumed at constant values. By monitoring and analyzing the frictional pressure drop (differential pressure between stations), termed Δp, both resistance and airflow evolutions can be inferred. If there is a ventilation interruption, it can be assumed that the resistance becomes *a* times its original value ($a \times R$) and the airflow becomes *b* times its original value ($b \times Q$). Then the corresponding frictional pressure drop becomes:

$$P_{ij} = \Delta p' = (ab^2)RQ^2 = ab^2\Delta p \tag{4-16}$$

For a continuous airway, *b* is a constant for the whole airway because of the continuity law holds for a continuous airway. However, *a* is a function of the position chosen for monitoring the pressures. If there is no ventilation interruption between positions *i* and *j*, *a* should be equal to unity because no resistance change will occur between position *i* and position *j*. If there is an actual ventilation interruption between position *i* and position *j*, *a* will change depending on whether resistance increases or decreases, and P_{ij} will therefore be influenced. Because frictional pressure drop is a position-dependent parameter, the pressure drop monitoring data can be used to identify the segment(s) where there are ventilation interruptions between different pressure monitoring stations. This conclusion has been confirmed by the SRCM field experiments and by the simulation results for the small and large mine case studies.

4.3.4.4 Pressure and velocity profiles in CFD model

Figure 4-30 shows the pressure and velocity profiles with respect to the various ventilation interruptions. Total pressure values are marked in Figure 4-30 (a), (c), (e), (g), and (i). In the CFD-modeled results, the monitoring stations are unmarked to avoid obscuring the results. Figure 4-21 can be used to locate the positions. Additionally, it should be noted that the pressure marked in Figure 4-30 is CFD-used pressure and does not correspond to the measured barometric pressures in the field. The pressures represent the relative values compared to the reference pressure. The established CFD model is a steady-state model to define the equilibrium conditions for various ventilation scenarios (defined in Section 4.3.2). In order to compare all the ventilation scenarios, the fixed pressure boundary was used for all the simulation, the inlet pressure was fixed at 380 Pa and the outlet pressure was fixed at 0 Pa.

For the condition of fully open at P2, pressure continuously dropped along the airflow direction because of the normal airway frictional pressure drop and shock loss (Figure 4-30 (g)). As expected, an abrupt pressure drop was observed across the regulator between P3 and P4 because of the high resistance of the regulator. After air went through the regulator, the total pressure became very low

and close to the total pressure at the return. When the cross-sectional area was reduced by blockage between P2 and P20, the resistance increased, and the pressure drop across the obstruction increased in turn. For example, when the open area was 80% of its original value, the differential pressure between P20 and P2 was 9.56 Pa. When the resistance between P20 and P2 was continually increased, the pressure drop correspondingly increased. When the open area was reduced to 50% and 10% of its original value, the pressure drop between P20 and P2 increased to 15.55 Pa and 138.65 Pa, respectively. These results suggest that there is a very large resistance increase when the open area is only 10% of its original value.

The pressure drop across the regulator was relatively high, ranging from 121.86 Pa to 199.01 Pa for most cases except the short circulation, because the resistance across the regulator sustained a constant high value. In the case of short circulation (Figure 4-30(i)), the major airflow from the intake directly flowed into the return through the short circuit airway between P4 and P6, i.e., the intake and return. Therefore, the pressure quickly dropped along the short circuit path. Very limited airflow went through the system and then passed through the regulator toward the return. There was minimal total pressure drop for the whole mine in this case because the overall resistance was minimal, as shown in Figure 4-30(i).

Similarly, the velocity profile of the CFD model is shown in Figure 4-30. According to Darcy's Law and Square Law, a higher-pressure gradient will cause higher air velocity for a cross-section area of a given shape. For the fully open condition illustrated in Figure 4-30(h), the highest velocity occurred at the regulator where the pressure gradient is the highest. However, unlike the pressure profile, the velocity profile is not a constant value at any given cross-sectional area. For this reason, the velocity measurement had a higher rate of error than pressure monitoring.

One reason for the unstable velocity was the localized turbulent flow, which is also shown in the figures as the turbulence energy. It can be observed that for the first corner in intake, although the velocity vector was evenly distributed at a certain plane, the turbulence energy was high at local positions. This will ultimately cause a higher localized velocity than the average velocity, leading to a measurement inaccuracy. Therefore, differential pressure is more reliable for monitoring ventilation interruptions in field measurement and is recommended for field monitoring. Upon reducing the opening area, the resistance between P20 and P2 increased and the velocity across the location correspondingly increased. This phenomenon is demonstrated in Figures 4-30(b), (d), and (f). Nonetheless, the turbulence-induced velocity instability can be observed in each case mentioned above. In the short circuit case, the highest velocity occurred at the stopping where the intake and return connect, which agrees with the pressure gradient results.

4.3.4.5 Differential pressure in CFD model

As with the field data, three sets of differential pressures were analyzed to determine the interruption location. P_{14} is the differential pressure between the intake and return, P_{34} is the differential pressure across the regulator, and P_{202} is the differential pressure across the airway blockage between P20 and P2. The results in Figure 4-31 agree with the field data's indication that the interruption locations can be identified from the percentage change of the differential pressures. The interruption-induced percentage change of differential pressure can be captured from the differential pressure between the intake and return because the system resistance will increase as the local resistance increases. Since no interruption occurred between P3 and P4, the differential pressure P_{34} only slightly varied, due to the limited airflow change based on the Square Law. If the interruption occurs between the monitoring stations, the differential pressure change can be significant, as shown in this example for P_{202}.

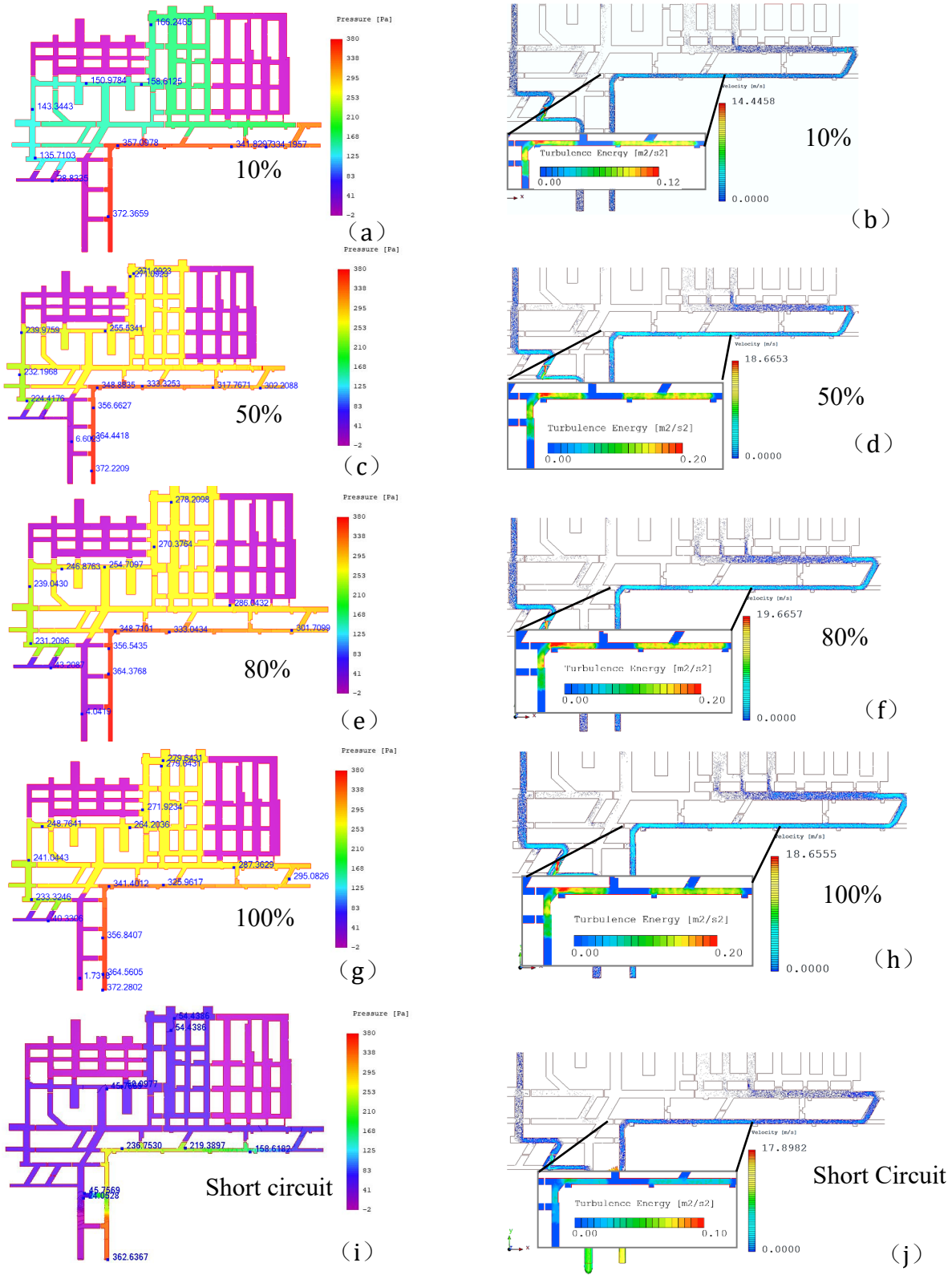

Figure 4-30. Pressure (Pa) and velocity profile with respect to various ventilation interruptions.

By comparison with the CFD model results, the location of the interruption can be determined from an excessive pressure change. In this study, the percentage change of differential pressure between P20 and P2 was much larger than that between other locations, as shown in Figure 4-31. Therefore, the CFD simulation results also confirm the field test results and demonstrate that differential pressures between limited monitoring positions are workable indicators for ventilation interruptions. Differential pressure monitoring can therefore provide helpful guidance for post-accident rescues and mine ventilation management if the pressure data is properly monitored and analyzed.

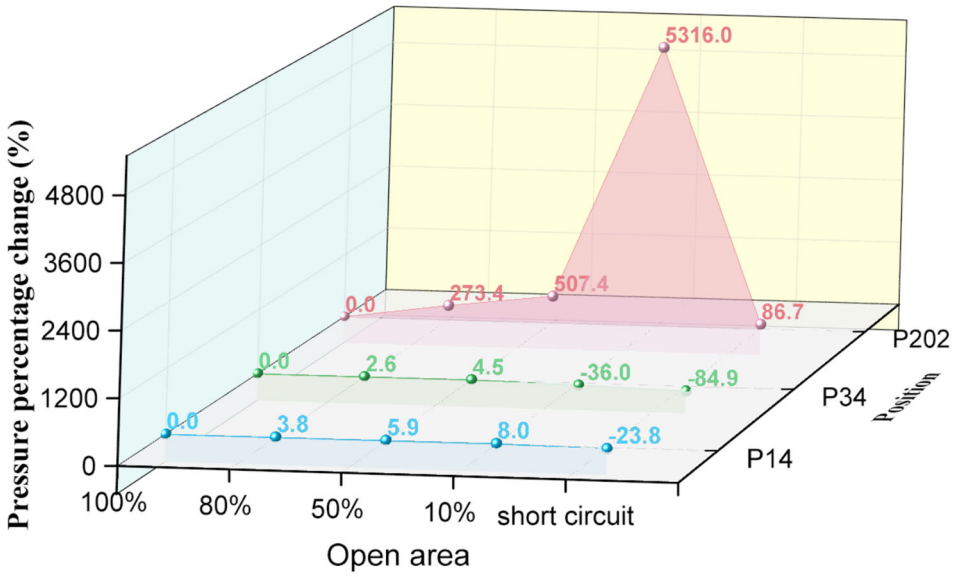

Figure 4-31. Pressure percentage change with respect to various ventilation interruptions.

4.3.5 Summary of the In-Mine Experiments and CFD Simulations

Pressure monitoring based atmospheric monitoring system can effectively capture the subsurface ventilation interruptions and serve as an early sentinel and precursor for ventilation interruptions. The following conclusions can be drawn from this study's field investigations and CFD simulations:

1) Pressure data is much more stable and reliable than velocity data for underground ventilation monitoring because localized turbulence can dramatically influence average velocity, making accuracy in velocity measurement difficult to achieve.
2) Differential pressure between various locations can be used as an index to capture ventilation interruptions and also to determine the location of the interruptions.
3) Effective sensor positioning can be achieved with a limited number of sensors. Localized ventilation interruptions can be identified by analyzing the differential pressure data.
4) Field investigation data and analyzing methods are supported by CFD simulation data. Velocity variations caused by turbulence are also well demonstrated in the CFD model.

5.0 Publication Record and Dissemination Efforts

The transfer of knowledge began recently when Dr. Jeffery Kohler gave a presentation at the 2019 annual SME conference titled "Strategic Location of Sensors in Atmospheric Monitoring Systems".

In the presentation, both airflow and pressure data from multiple mines were presented and discussed.

For future dissemination plan, an additional peer reviewed journal paper is expected to be written and submitted. This paper will also include the maps, figures, and data gathered from the work conducted in the mines. Finally, another abstract will be submitted for presentation to the 2020 annual SME conference. These two presentations and potential peer reviewed journal article will provide the mining community with sufficient means to understand and appreciate the research conducted at Penn State under this Alpha foundation grant.

6.0 Conclusions and Impact Assessment

Advances in technology enabling economic and reliable communications, miner tracking, and remote monitoring of mine conditions since the passage of the MINER Act have positioned the industry to achieve significant improvements in mine safety. However, one technology, atmospheric monitoring systems (AMS), has failed to gain acceptance despite its potential to prevent future mine disasters. Certainly, AMS is being applied for mandated fire monitoring and to satisfy other statutory requirements, including when belt air is used for intake. These applications, while important in their own right, fall short of the potential of this technology to save lives.

Monitoring technology for production and maintenance-related purposes has been embraced and is commonly employed in underground mines to realize significant productivity benefits. This is the case not because productivity is valued more than safety, but because there is a clear value proposition for one over the other. This is a problem that has persisted from the earliest days of mine-wide monitoring systems. Sensors and systems were costly to install and even more costly to maintain. These systems generated vast quantities of data that no one could use. Given this reality, why would anyone embrace this technology?

This research project took aim at this longstanding problem with the simple and straightforward goal of identifying the smallest number of sensors practicable to act as sentinels in an early warning system. A sensor location strategy was formulated and validated with computer simulations and in-mine experiments. The computer simulations were based on validated mine ventilation models of operating mines. In addition to the sensor location strategy, another major contribution of this research is the establishment of pressure as a superior surrogate to air velocity for monitoring air flow (quantity).

6.1 Pressure as a Sentinel

The state of the mine ventilation system is defined primarily by the direction and quantity of airflow throughout the mine. Historically, air velocity was monitored and used as a surrogate measure for air flow. As explained in Section 4.1.2, pressure is significantly more sensitive to changes in flow and is relatively unaffected by the confounders that affect air velocity measurements. Further, pressure transducers require less attention for maintenance and calibration. Consequently, it is recommended that pressure transducers be used as a sentinel rather than air velocity.

The installation is also simplified in that the pressure transducer can be located conveniently in fresh air, in most cases, and rubber tubing can be used to connect the desired monitoring spot to the pressure transducer. This may also simplify connection of the transducer to the mine's communication backbone. Either differential or absolute transducers can be used. In many cases a

differential transducer is the obvious choice and may be less costly than purchasing two absolute transducers and then calculating the difference between two pressures. For example, measuring the pressure drop across a regulator is easily accomplished with a differential transducer. In other cases, where the pressure at a location is of interest and will be compared to pressures in other, far-removed, parts of the mine, absolute transducers are the better choice. Pressure transducers with the appropriate characteristics are readily available commercially for a few hundred to a few thousand dollars depending on the sensitivity required. One such differential transducer is shown in Appendix II.

6.2 Location Strategy

The objective is to place sensors that will serve as early-warning indicators of potential or developing problems. The focus is on detecting these situations before they would be readily apparent to those working in the mine. These sensors would serve as sentinels, detecting the potential issue and alerting mine personnel. It is not intended that the sentinels will provide the information to diagnose the cause nor pinpoint the location of the disturbance. Rather, human intervention will be required to locate exactly the source of the disturbance and to diagnose the cause. Certainly, the addition of more sensors could further aid in more exact location and diagnosis, but this would defeat the purpose of the location strategy. Human intervention is going to be required in any case, and the marginal benefit of this additional information does not justify the cost of acquiring it.[10]

An adequate quantity of air, as defined by the engineering design and MSHA-approved mine ventilation plan, is critical to ensure the safety of mineworkers. If the quantity begins to deviate from plan values, then there is a cause to investigate further. As such, air quantity, or its pressure or velocity surrogate, is well suited to serve as a sentinel. The only situation in which a different sentinel is required to detect an incipient problem is leakage from a sealed area that is adjacent to active main or submain entries. For this purpose, a methane sensor is the appropriate sensor to serve as a sentinel.[11]

For specific locations, the following strategies are recommended:

- *Continuous miner sections.* The pressure across the section regulator should be monitored for each CM section.

- *Longwall sections.* The behavior of the airflow at the T-split is critical, as it is imperative that there is adequate air flowing from the tailgate entry to the bleeder entry. This condition can be monitored with one differential pressure transducer, which is illustrated in Figure 4-6 and Figure 4-17. There is value in monitoring the pressure across the tailgate regulator located near the mouth of the panel. These two sentinels should be adequate for most longwalls in the U.S. Certain unique practices to ventilate longwall sections are known to be

[10] It is not the intent here to discourage the use of additional sensors. Sensors at all of the evaluation points in the mine ventilation plan, for example, would certainly better inform decisions. However, would this additional information improve on the sentinel concept using minimal sensors recommend in this report? Would the cost of acquiring this information be offset by the value of the additional information acquired? The authors would answer *no* to both questions.

[11] As explained earlier in this report, the use of AMS to detect combustion is well established and used throughout the industry, as required by statute. Although not perfect, the current practice is reasonably effective. Accordingly, sentinels for detecting combustion were not considered in this project.

necessary. While the sentinels recommended here would still apply, consideration can be given to using an additional sentinel based on a local practice.

- *Sealed areas adjacent to active return airways*. Modern seal construction and installation practices should preclude significant leakage from sealed areas into active workings. Nonetheless, given the potential consequences of an undetected leakage, it is recommended that methane be monitored in the adjacent return aircourse outby the seals.

- *Junctions of panels, submains, and mains.* Sensors could be placed at junctions to facilitate a more exact determination of the location of a developing problem, rather than serving as sentinels. There may be a concern in a particular mine that would justify adding sensors at one or more junctions, but in most cases the information obtained is likely to contribute little to identifying the root cause of a ventilation disturbance, beyond that obtained from the sentinels.

- *Main fan.* It is common practice in mines today to remotely monitor parameters at the fan. Pressure and methane concentration are of particular interest as they can serve as sentinels. As such, it is recommended that these be included in the set of sentinels that would serve as an early-warning system for incipient problems affecting the mine ventilation system.

6.3 Routine and Post-Accident Application

The location strategy as presented is focused on routine operations in the mine. A catastrophic event, such as a mine explosion, massive ground collapse, or an inundation, but especially an explosion, increases the need for information. The location of the catastrophic event and the extent of collateral damage to ventilation controls, for example, are of urgent interest to those on the surface and underground alike. The availability of information from sensors will depend in large part on the survivability of the mine's communications infrastructure. The pressure sensors and hardened methane sensors comprising the sentinels are survivable and will continue to provide information as long as they remain powered and connected to the communications backbone, unless they happened to be located very close to the explosion. The information provided by the sentinels will be useful for assessing the post-event status of the ventilation system. This will be helpful to miners endeavoring to escape, if they have access to it, and to surface personnel who may need to mount a rescue effort. However, by limiting the number of sentinels to the smallest practical number and not placing them at junctions, for example, the value of the proposed early-warning system will be limited in a post-accident scenario.

6.4 System Characteristics

The sentinels should be polled once per minute, and it is recommended that a smoothing algorithm such as the Lowess Algorithm be applied to signals. Alarm or trigger levels for the sentinels will be determined by the design characteristics of the mine ventilation system and approved plan. It is recommended that the deadband around the trigger level be significantly reduced from historical practices of 25% to no more than 10%, i.e., ±5% of the trigger level, because the random fluctuations in pressure are found to be far less than those of velocity. The pressure transducer described in Appendix II was used in this project. Its resolution and accuracy are well in excess of that needed for use as sentinels in the manner described in this report. The 5-psi model, for example, has a resolution of 0.01" w.g. (2.5Pa). This is far more sensitive than would ordinarily be required. The precision of this unit is also excellent.

7.0 Recommendations for Future Work

The strategic location of sensors to form an early-warning system is ready for implementation. Notwithstanding, a demonstration project in an operating mine would serve as a real-world validation of the early-warning concept. Additionally, the following research directions could be explored to build on this project's findings:

1) In-depth analysis of the pressure variations at different ventilation controls in addition to mine regulators would be helpful. Future research might study, for example, the pressure in the longwall gob as the longwall retreats. This work might generate insights on the potential movement of gas from the gob to the face.
2) Research to improve the utilization of real-time surface-weather information in ventilation pressure analysis would be useful. The effects of seasonal and daily variations of surface atmospheric temperature and humidity are known, but the expected impact on the pressure profile in underground mine, and specifically the choice of a deadband for this early warning system, are not fully known.
3) Research to develop cost-effective methods to capture and quantify excessive airflow leakage would be beneficial for mine operators. Although pressure-based monitoring can serve as a sentinel to determine the ventilation interruption at primary aircourses, it is unable to capture normal levels of airflow leakage.
4) Application of this study's findings to non-coal mines should be tested and evaluated. For example, one challenge for large-opening mines is directing the air to different headings. If a pressure-based monitoring system can provide information guiding changes to the ventilation controls, this capability would be very beneficial for other commodities extracted from large-opening mines, such as salt, lead, zinc and limestone.

8.0 Acknowledgement

This study was sponsored by the Alpha Foundation for the Improvement of Mine Safety and Health, Inc. (Alpha Foundation). The views, opinions and recommendations expressed herein are solely those of the authors and do not imply any endorsement by the Alpha Foundation, its Directors and staff. Mention of any company name, product, or software does not constitute endorsement by the Alpha Foundation or The Pennsylvania State University. The authors gratefully acknowledge the Alpha Foundation for the support of this mine safety research, which would not have been possible without funding from the Foundation.

Current and former mining professionals from industry and government, too numerous to mention here, graciously answered our many questions and provided valuable input to this research. Two underground coal mines allowed our researchers access to their mines to collect data, despite the significant pressures under which underground coal mines are operating. Regrettably these mine operators prefer to remain anonymous, but their support of mine safety research, even in these difficult times, is crucial to the success of mine safety and health research.

The authors gratefully acknowledge Don Knuckles and Brad Coates, among others at Matrix Team, for their interest in improving mine safety and for the loan of sensors and AMS system components to support the in-mine efforts of this project.

Terry Theys, retired from Alpha Natural Resources (ANR), was an early advocate for this research. His work in collaboration with Matrix Team to develop and install AMS in many Alpha Natural

Resources' mines resulted in the most significant demonstration of the potential of AMS to do so much more to improve mine safety than had been previously considered.

Finally, the authors acknowledge Professor Kray Luxbacher, Virgina Tech, and Professor Zach Agioutantis, University of Kentucky for their willingness to share data and ideas in an effort to facilitate broader application of AMS to improve mine safety.

9.0 References

Agioutantus, Z., Luxbacher, K., Karmis, M., & Schafrik, S. (2014). Development of an atmospheric data management system for underground coal mines. Journal of the Southern African Institute of Mining and Metallurgy, 114(12), 1059-1063.

Cohen, A., Fisher, T., & Kohler, J. L. (1987). Location strategy for methane, air velocity, and carbon monoxide fixed-point transducers. IEEE Transactions on Industry Applications, IA-23, 375-381.

Danko, G. L. (2013). Subsurface flow and transport process model for time dependent mine ventilation simulations. Mining Technology, 122(3), 134-144.

Griffin, K. R., Jong, E. C., Luxbacher, K. D., & Westman, E. C. (2011). A review of atmospheric monitoring systems in underground coal mines: Implications for explosion prevention. SME Annual Meeting, 683-686.

Kohler, J. L. (1986). The characteristics of mine airstreams and special considerations for mine monitoring. Proceedings of the 3rd Mine Ventilation Symposium, 175-181.

Kohler, J. L., & Thimons, E. D. (1987). An analysis of air volume-flowrate determinations for mines. Mining Science and Technology, 6, 17-29.

Kohler, J. L. (1987). Conceptual investigation of a management information system for underground coal mines. NTIS PB87-188736, Bureau of Mines, 229 pp.

Kohler, J. L. (1992). Monitoring, control, and communications. In H. Hartman (Ed.)., SME Mining engineering handbook (2nd ed.) (ch. 12.6). Littleton, CO: Society for Mining Metallurgy.

Litton, C. D., & Perera, I. E. (2015). Evaluation of sensors for mine fire detection using an atmospheric monitoring system. Mining Engineering, 68-75.

McElroy, G. E., & Kingery, D. S. (1957). Making ventilation-pressure surveys with altimeters. Washington, D.C.: U.S. Department of the Interior, Bureau of Mines.

McPherson, M. J. (1993). Subsurface ventilation engineering. Retrieved from http://www.mvsengineering.com/

Sasmito, A. P., Birgersson, E., Ly, H. C., & Mujumdar, A. S. (2013). Some approaches to improve ventilation system in underground coal mines environment - A computational fluid dynamic study. Tunnelling and Underground Space Technology, 34, 82-95.

Wala, A. M., Jacob, J. D., Rangubhotla, L., & Watkins, T. (2005). Evaluation of an exhaust face ventilation system for a 6.1-m (20-ft). Mining Engineering, 57(10), 33.

Wala, A. M., Vytla, S., Taylor, C. D., & Huang, G. (2007). Mine face ventilation: A comparison of CFD results against benchmark experiments for the CFD code validation. Mining Engineering, 59(10), 49-55.

Xu, G., Luxbacher, K. D., Ragab, S., & Schafrik, S. (2013). Development of a remote analysis method for underground ventilation systems using tracer gas and CFD in a simplified laboratory apparatus. Tunnelling and Underground Space Technology, 33, 1-11.

Xu, G., Jong, E. C., Luxbacher, K. D., & Mcnair, H. M. (2015). Effective utilization of tracer gas in characterization of underground mine ventilation networks. Process Safety and Environmental Protection, 99, 1-10.

Xu, G., Jong, E. C., Luxbacher, K. D., Ragab, S. A., & Karmis, M. E. (2015). Remote characterization of ventilation systems using tracer gas and CFD in an underground mine. Safety Science, 74, 140-149.

10.0 Appendices:

Appendix I: Data Acquisition System

A1.1 Pressure Measurement

A pressure recording system was constructed to continuously monitor and record the pressure data in the mine environment, as illustrated in Figure 10-1.
Figure 10-1 shows the developed prototype instrument used to monitor and record all the barometric pressure data collected in lab and field experiments. Two high-accuracy Setra Model 270 barometric sensors, labeled ② in Figure 10-1, were installed on the prototype unit. The Model 270 is Setra's best performing analog sensor for barometric pressure measurement. The features of these two installed sensors include a high-accuracy analog sensor (±0.03% FS); capturing the dynamic pressure changes with high frequency; a stable ceramic sensor for robust severe weather detection; repeatability within 0.01% FS; excellent long-term stability (0.1% FS/YR); low power consumption; instant warm-up; and fast response time. The two most important features for in-mine use are the high accuracy and low power consumption, allowing the unit to be installed in the mine for a long period time to monitor subtle pressure changes. For this unit, the T&D MCR-4V data logger was used for pressure logging and recording on a SD card, labeled ③ in Figure 10-1. The unit is equipped with a TDK-12Vdc power supply, labeled ④ in the figure. This power supply provides enough power to the barometric pressure sensors for at least two weeks of continuous monitoring and recording of pressure data. The wiring schematic of this pressure monitoring system is shown in Figure 10-2. Tygon tubing can be connected to the pressure sensors to provide a pathway to the designated measurement stations.

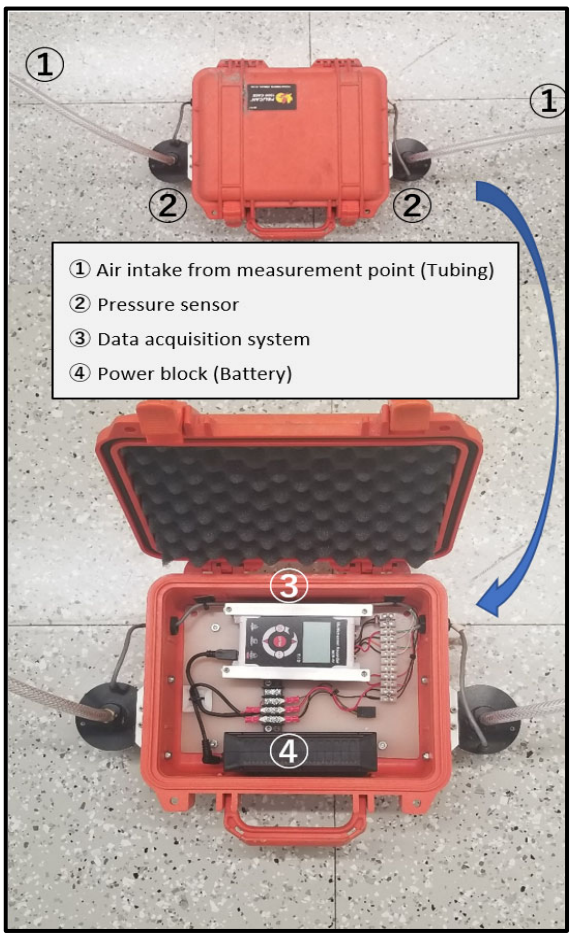

Figure 10-1. Pressure monitoring and recording system.

This developed unit was tested at Penn State Mine Ventilation Laboratory (PSU-MVL) for its accuracy and reliability. The unit was installed to measure the differential pressures at different locations at the NIOSH Safety Research Coal Mine, as illustrated in Figure 10-3.

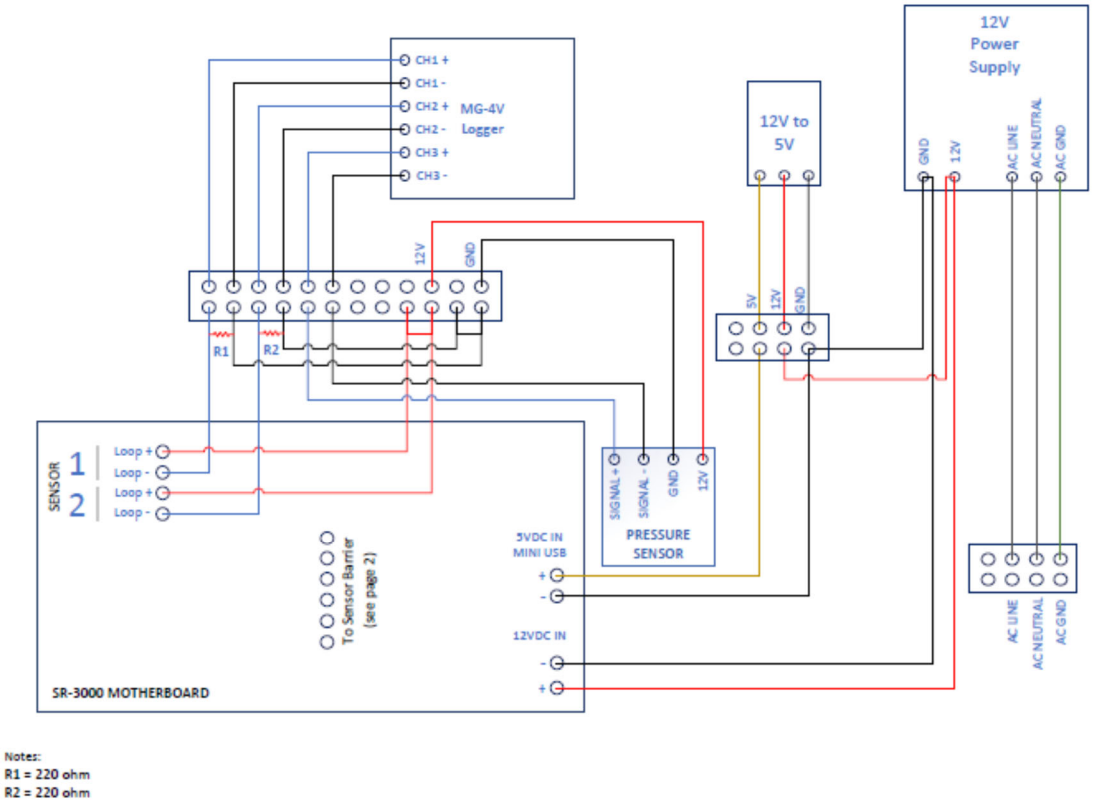

Figure 10-2. Pressure monitoring and recording system wiring schematic.

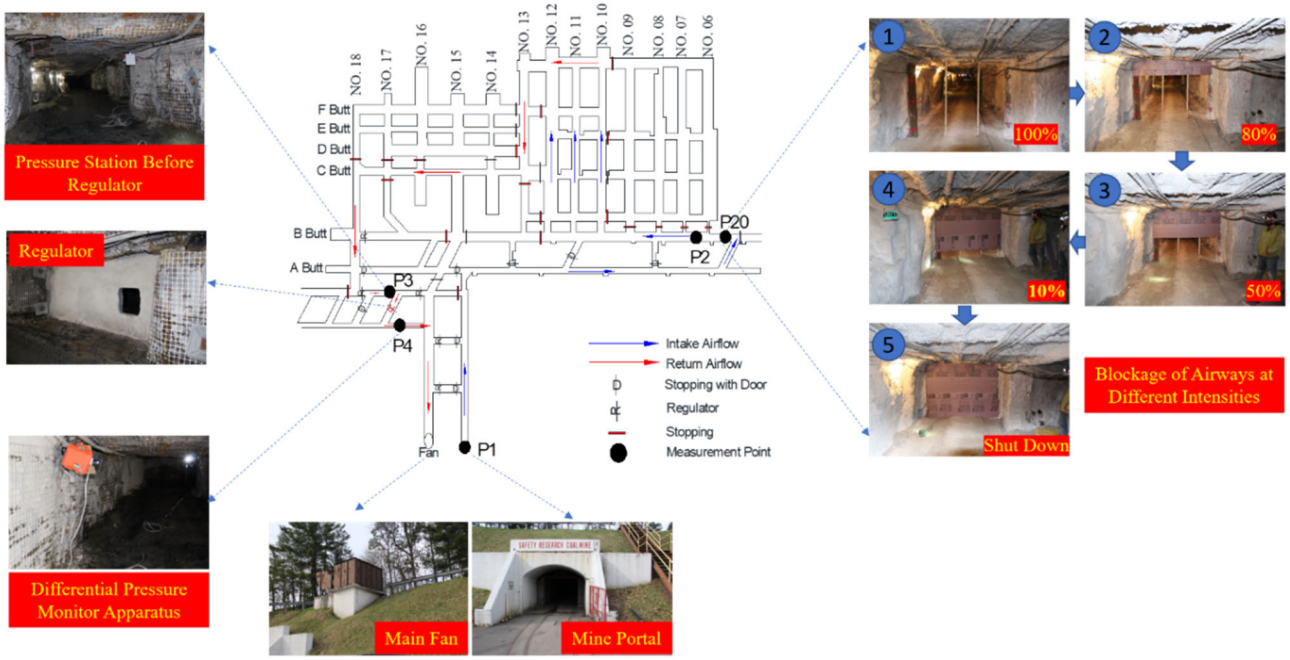

Figure 10-3. Safety research coal mine layout and ventilation monitoring stations.

A1.2 Velocity Measurement

An air velocity recording system was constructed to continuously monitor and record velocity data in the mine environment, as illustrated in Figure 10-4.

Figure 10-4 shows the developed prototype instrument used for this purpose. The ultrasonic velocity sensor from Matrix Design Group LLC was used for the prototype development. The Matrix ultrasonic velocity sensor recorded velocity values at a frequency of 20 HZ. As shown in Figure 10-4, the velocity was measured using the ultrasonic velocity sensor, labeled ②, and the data transmitted through the electrical breaker box, labeled ③. Then data can be transferred to the data acquisition and recording system, labeled ①. Results can be instantaneously read from the digital display on box ① while all results are stored on a removable SD card. The wiring schematic of this velocity monitoring system is shown in Figure 10-5. This velocity measurement prototype was tested in the PSU-MVL for its reliability and accuracy, as shown in Figure 10-4.

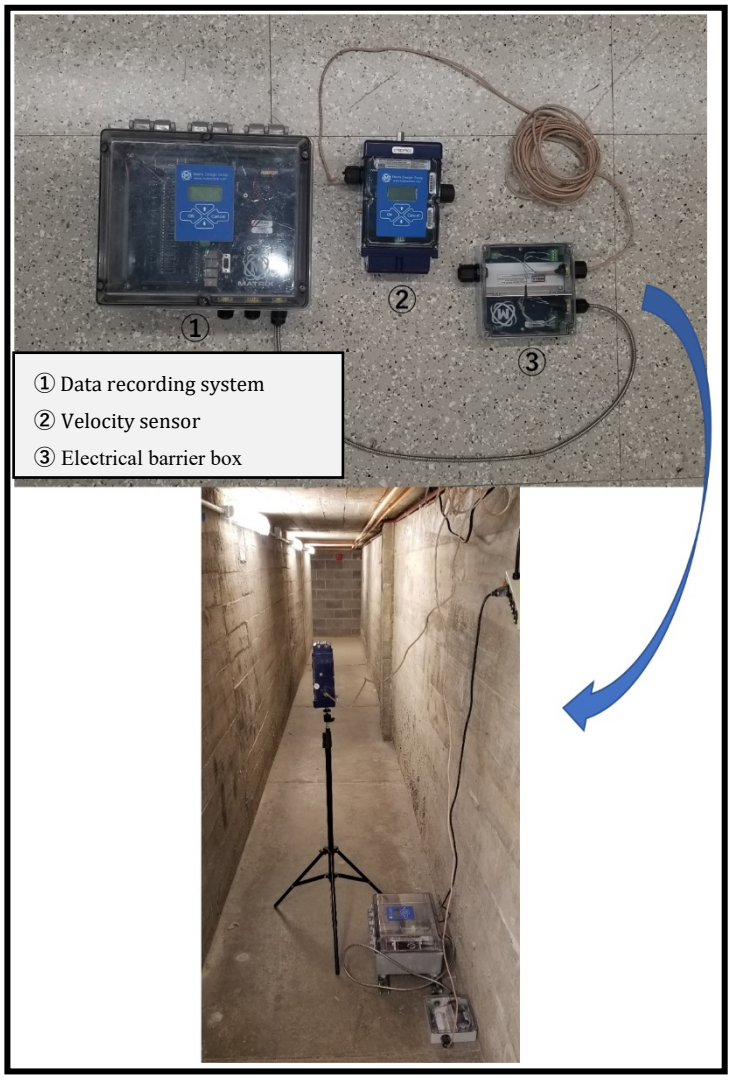

Figure 10-4. Airflow velocity system installed in the PSU-MVL.

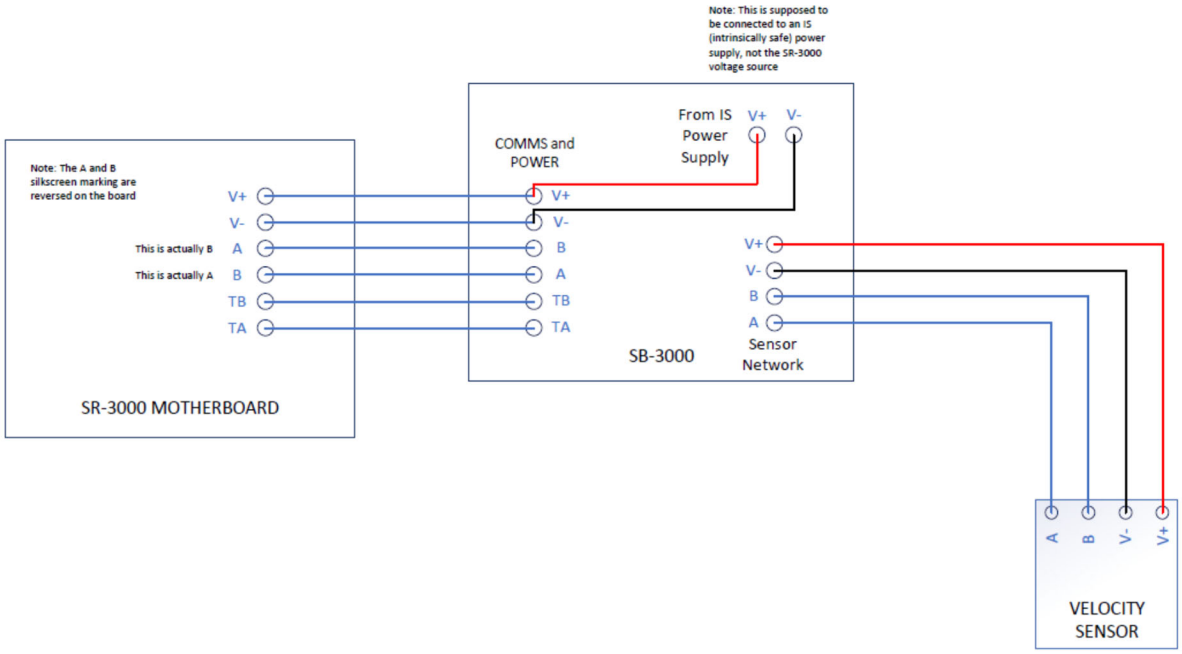

Figure 10-5. Velocity monitoring and recording system wiring schematic.

Appendix: II: Setra Pressure Transducer

Specification of Sensor: The Model 270 is Setra's best performing analog sensor for barometric pressure measurement. The features of these two installed sensors include a high-accuracy analog sensor (±0.03% FS); capturing the dynamic pressure changes with high frequency; a stable ceramic sensor for robust severe weather detection; repeatability within 0.01% FS; excellent long-term stability (0.1% FS/YR); low power consumption; instant warm-up; and fast response time. The two most important features for in-mine use are the high accuracy and low power consumption, allowing the unit to be installed in the mine for a long period time to monitor subtle pressure changes.

In-mine Pressure Monitoring Capability: The Setra Model 270 barometric pressure sensor has the accuracy of ± 50 psi × 0.03% = ± 0.015 psi (~2 Pa). Because of its high accuracy, the sensor can provide a reliable barometric pressure at each measuring point. The differential pressure can then be computed between two measuring points using this high accurate barometric sensor. Based on the details in Section "*4.1.3 Sensor Location Strategy*", the differential pressure between the sensing location are always greater the order of magnitude of two or more. Therefore, Model 270 barometric sensor can provide accurate and sensitive enough pressure data for the ventilation monitoring.

The detailed specifications of the Setra sensor is attached in next two pages.

Model 270

SETRACERAM™ for Barometric, Gauge or Absolute Pressure

The Model 270 is Setra's highest performing analog sensor for barometric, absolute and gauge pressure measurements. Its decades worth of installations have built a reputation of reliability and remains the trusted choice for critical installations. The ceramic sensor on the 270 delivers high performance; its ±0.03% FS accuracy over a wide temperature range outperforms competitive transducers in the environmental sensing market. The 270 offers multiple options to fit the needs of difficult applications, making it easier to install and gather higher quality data for your project.

High Accuracy For Demanding Applications

The Model 270 pressure transducer is the most accurate analog sensor Setra manufactures. The available 0.03% FS accuracy is perfect for vital installations where precise measurements determine success or failure of the application.

Improved Performance With Ceramic Sensor

The 270 utilizes a variable capacitance sensor that is made using ceramic material fused together with glass and gold to form the SETRACERAM™ pressure element. This stable material and design offers class leading thermal performance and low hysteresis, allowing integration into demanding installations. The ceramic sensor enables improved performance compared to other stainless steel sensors, enabling the 270 to give accurate measurements and better test results.

Flexibility in Installation

The 270 offers mechanical and electrical options that can be installed into existing applications. These options reduce engineering design time, allowing for earlier project completion.

- **Highest Accuracy Analog Sensor**
- **Captures Dynamic Pressure Changes**
- **Robust For Severe Weather Detection**

Model 270 Features:

- High Optional Accuracy: ±0.03% FS
- Stable Ceramic Sensor
- Repeatability Within 0.01% FS
- Excellent Long-Term Stability: 0.1% FS/YR
- Low Power Consumption
- Instant Warm-Up
- Fast Response Time

Applications:

- High Accuracy Barometric Pressure Measurement
- Weather and Environmental Data
- Data Buoys and Remote Weather Stations
- Engine Test Cells

Phone: 800-257-3872 • Fax: 978-264-0292 • setra.com

Model 270

SETRACERAM™ for Barometric, Gauge or Absolute Pressure

ORDERING INFORMATION

2 7 0 1 – ☐☐☐ – ☐ – ☐ – ☐☐ – ☐☐ – ☐☐ – ☐ – ☐☐

Model	Pressure Range		Units		Pressure Type		Fitting		Output		Termination		Accuracy		Options	
2701 = 270	600	600-1100	M	mb/hPa	A	Absolute	1F	1/8" NPT Internal	2B	0 to 5 VDC (24 VDC EXC)	02	2' Cable	N	±0.05% FS	NN	None
	800	800-1100	M	mb/hPa	G	Gauge (PSI units only)			3B	0 to 5 VDC (12 VDC EXC)	10	10' Cable	Y	±0.03%[2] FS	C	11 PT Cal. Certificate
	005[1]	0-5	P	PSI							25	25' Cable			D	Mate with Datum
	010	0-10	P	PSI							XX	Consult facotry for other cable lengths			F	Nema 4 Enclosure
	020	0-20	P	PSI											L	Etched SS Tag
	050	0-50	P	PSI											2	-13 to 150°F Compensated Range[2]
	100	0-100	P	PSI												

[1]Available in Gauge Pressure Type Only
[2]Accuracy "Y" and Option "2" cannot be combined

Example: Part No. 2701800MA1F2B02YNN = Model 270, 800-1100 mb/hPa pressure range, Absolute, 1/8" NPT internal fitting, 0 to 5 VDC Output, 2' Cable Length, ±0.03% FS Accuracy.

Both boxes must be filled in alphanumeric order:
- If No options: N + N
- If 1 option: Option Code + N
- If 2 options: Option Code + Option Code

DIMENSIONS

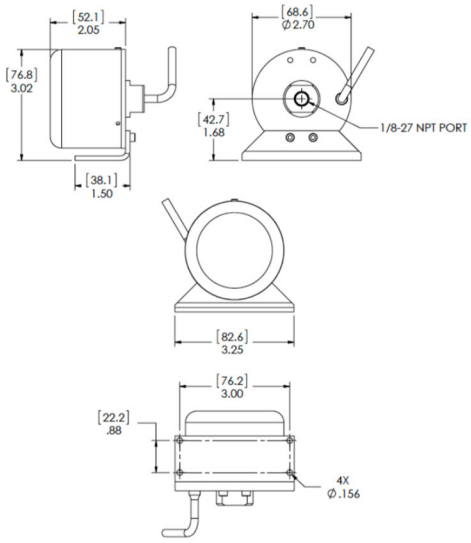

PROOF PRESSURE

Type of Pressure	Pressure Range	Maximum Pressure
Barometric	600 to 1100 hPa/mb 800 to 1100 hPa/mb	20 psia
Absolute	0 to 10, 20, 50, 100 psia	1.5 x rated
Gauge	0 to 5, 10, 20, 50, 100 psig	1.5 x rated

GENERAL SPECIFICATIONS

Performance Data		Environmental Data	
Accuracy RSS[1] (at constant temp)	±0.05% FS	Temperature	
Non-Linearity		Operating °F(°C)	0 to +175 (-18 to +80)
End Point	±0.05% FS	Storage °F(°C)	-65 to +250 (-54 to +120)
Best Fit Straight Line	±0.03% FS	Vibration	2g from 5Hz to 500 Hz
Hysteresis	<0.01% FS (TYP.)	Acceleration	10g
Resolution	Infinite, limited only by output noise level (0.005% FS)	Shock	50g Operating, 1/2 sine 10ms
Thermal Effects[2]		Pressure Fitting	1/8"-27 NPT Internal
Compensated Range °F(°C)	+30 to +120 (-1 to +49)	Electrical Connection	2' Multiconductor Cable
Thermal Zero Shift %FS/°100F (%FS/50°C)		Weight (approx.)	9 ounces (0.25 Kgm)
Barometric	±0.2 (±0.18)	**Electrical Data**	
Other Ranges	±0.1 (±0.09)	Electrical Circuit[3]	4-Wire (+Exc, -Exc, _Out, -Out)
Thermal Coefficient Sensitivity	±0.1 (±0.09)	Excitation[4]	24 VDC (22-32 VDC) 12VDC (11-15 VDC) Reverse Wiring Protection
Long Term Stability	< ±0.1% FS/YR		
Warm-Up	< ±0.04% FS shift after 20 minutes at constant temp.	Output[5]	0 to 5 VDC[6]
Time Constant	<10 milliseconds to reach 90% final output with step function pressure input	Isolation	The insulation resistance between all signals leads tied together and case ground is 100 ohms minimum at 25 VDC
Pressure Media		Output Impedance	<5 ohms
Non-condensing air or gas compatible with hard anodized aluminum, alumina ceramics, gold, fluorocarbon elastomer sealant & Buna-N O-Ring.		Output Noise	<200 microvolts RMS (0 Hz to 100 Hz)
		Current Consumption	8 mA (0.2 Watts)
Approvals			
CE			

[1]RSS of Non-Linearity, Hysteresis, and Non-Repeatability. Higher accuracy units available on special order.
[2]Units calibrated at nominal 70°F. Max thermal error computer from this datum.
[3]For best performance, either negative excitation or negative output should be connected to case (ground). Both leads cannot be connected to case (ground). Units calibrated at the factory with negative excitation connected to case.
[4]Internal regulation minimizes effect of excitation variation, with <±0.005% FS output change. Will operate on 28 VDC aircraft power per MIL-STD-70A and not be damaged by emergency power conditions.
[5]Calibrated into a 50K ohm load, operable into a 5000 ohm load or greater.
[6]Zero output factory set to within ±5mV. Span (Full Scale) output factory set to within ±5mV.

SS270 REV. F 10/16

Phone: 800-257-3872 • Fax: 978-264-0292 • setra.com